New Perspectives in Spintronic and Mesoscopic Physics Symposium @Kashiwa
2015.06.12

Conversion from a charge current into a spin polarized current in the surface state of three-dimensional topological insulator

○Yuichiro Ando[1], Satoshi Sasaki[2], Kouji Segawa[2], Yoichi Ando[2], and Masashi Shiraishi[1]

1. Department of Electronic Science and Engineering, Kyoto University
2. Institute of Scientific and Industrial Research, Osaka University

Y. Ando et al., Nano Lett. 14, 6226(2014).

Acknowledgments

Osaka Univ.

Fabrication of TI

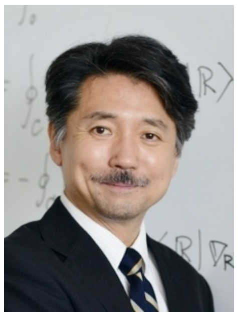

Prof. Yoichi Ando

Prof. Kouji Segawa

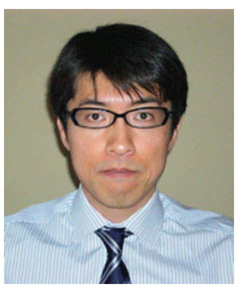

Dr. Satoshi Sasaki

Dr. Fan Yang

Dr. Mario Novak

Kyoto Univ.

Detection of spin current

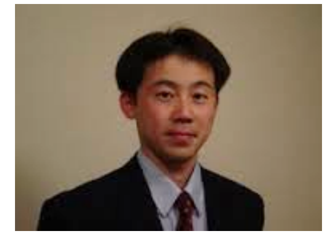

Prof. Masashi Shiraishi

Mr. Takahiro Hamasaki

Mr. Takayuki Kurokawa

The surface state in 3D topological insulator

Surface state of topological insulator

- ✓ 2D metallic surface state
- ✓ Dirac electron system

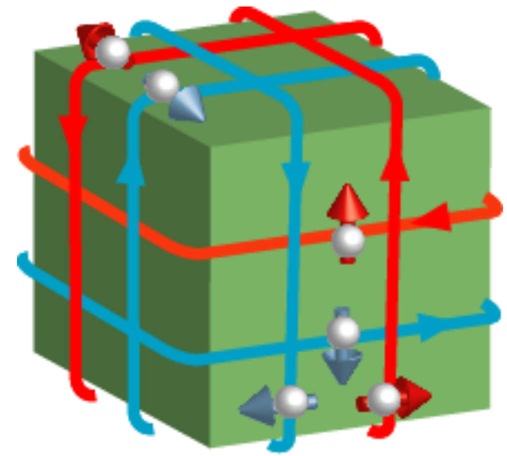

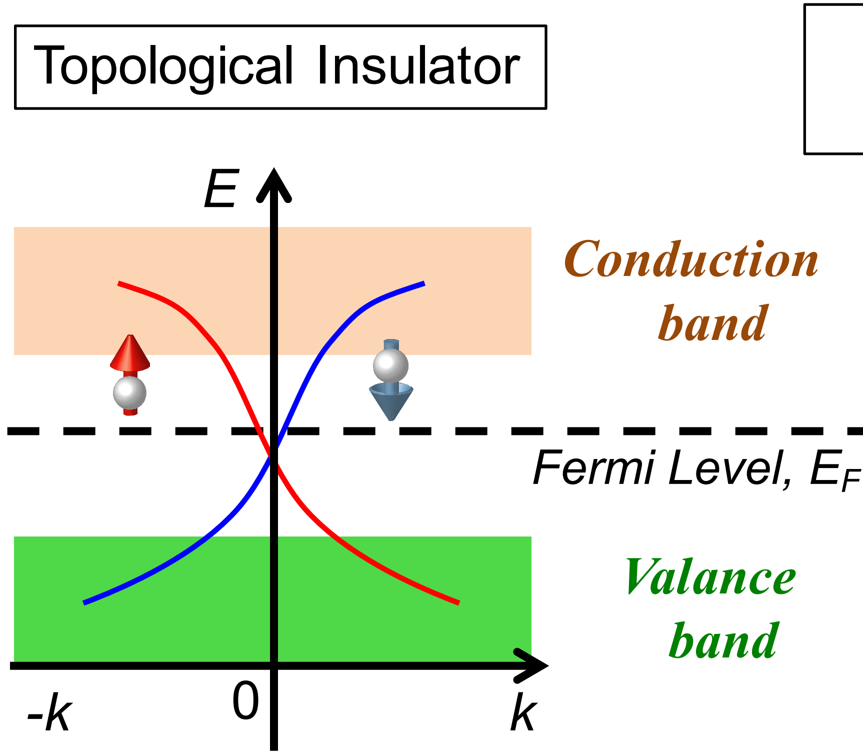

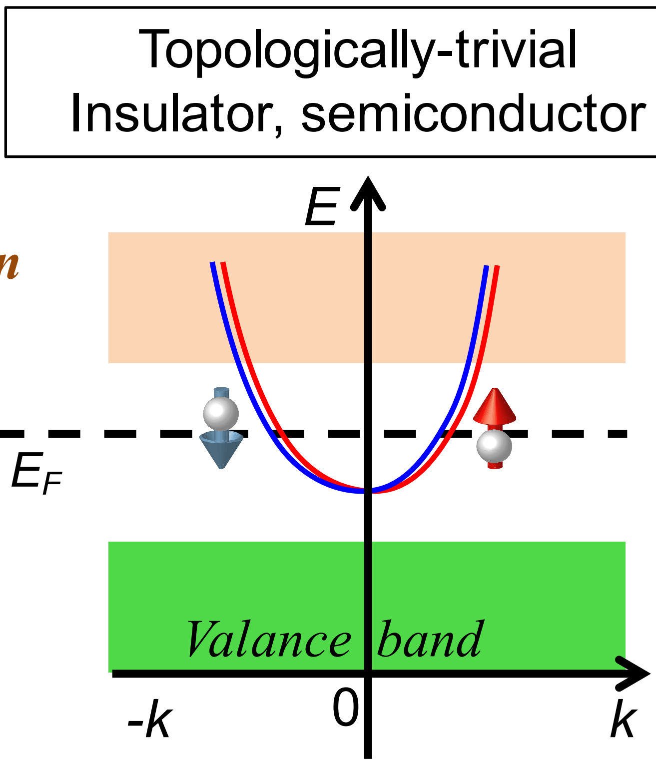

Spin-momentum locking in 3D topological insulator

Surface state of topological insulator (TI)

✓ 2D metallic surface state
✓ Dirac electron system

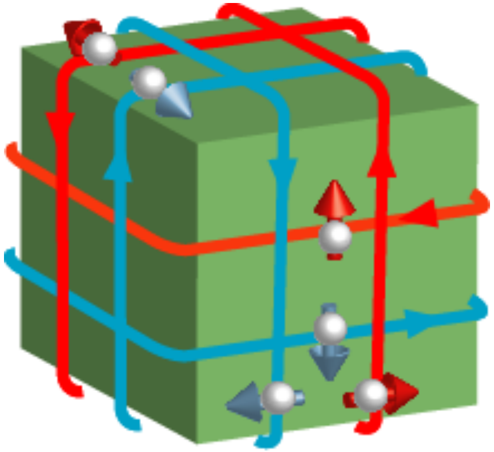

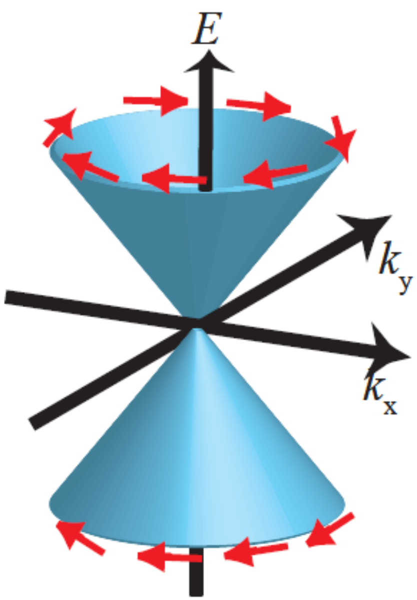

"*Spin-momentum locking*"

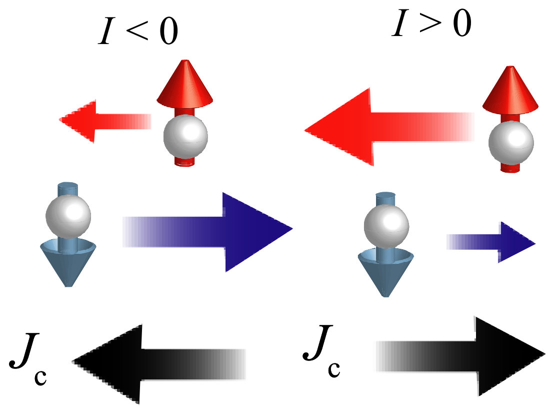

Objective

Electrical injection/extraction of the spin polarized current due to charge flow in the surface state of the topological insulator

Verification of surface state of 3D topological insulator

Band structure of surface

(Angle-Resolved Photo Emission Spectroscopy)

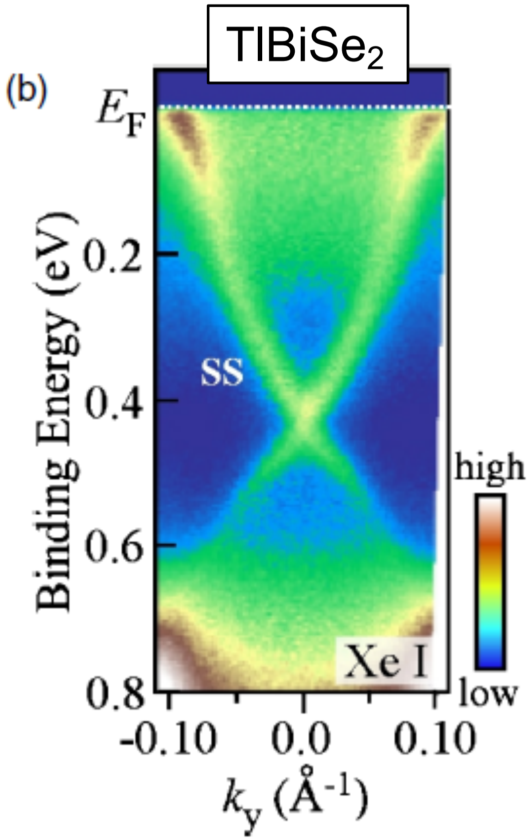

T. Sato et al., Phys. Rev. Lett. **105**, 136802 (2010).

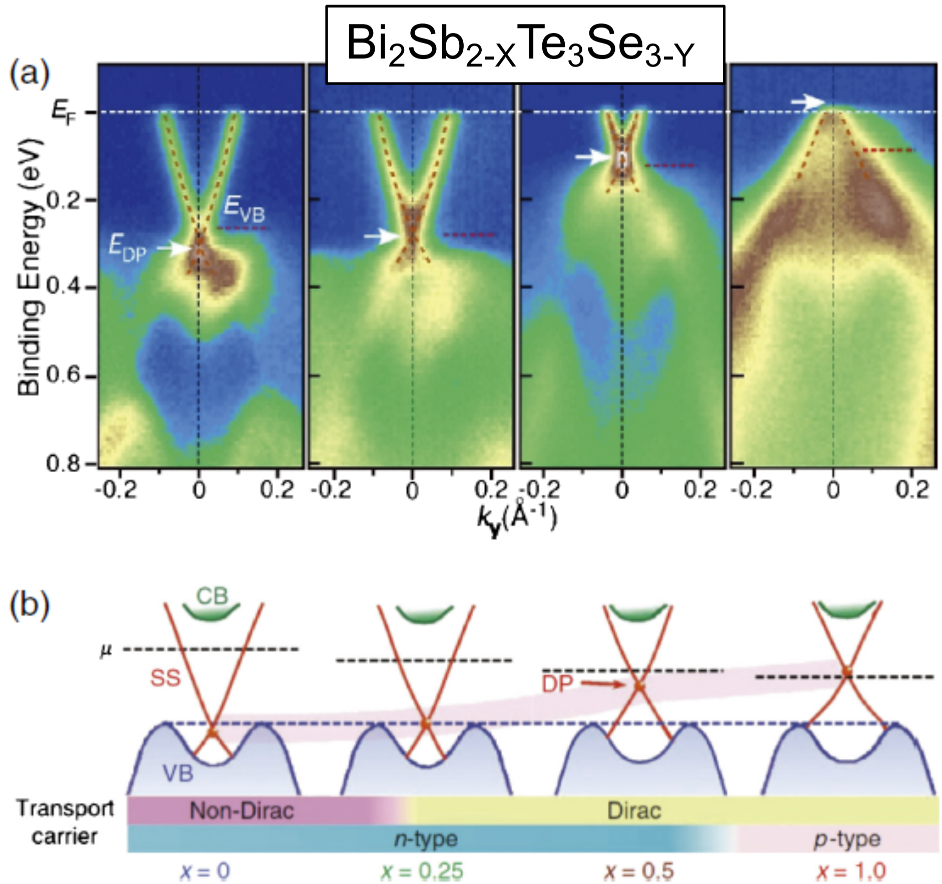

T. Arakane et al., Nat. Comm. **3**, 636 (2012).

Verification of surface state of 3D topological insulator

Two dimensional transport properties

Shubnikov-de Haas oscillations

Bi_2Te_2Se

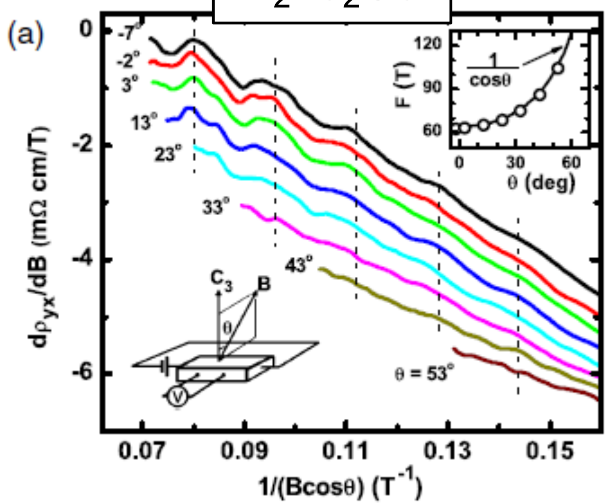

Z. Ren et al., Phys. Rev. B **82**, 241306(R) (2010).

Bi_2Se_3 thin film

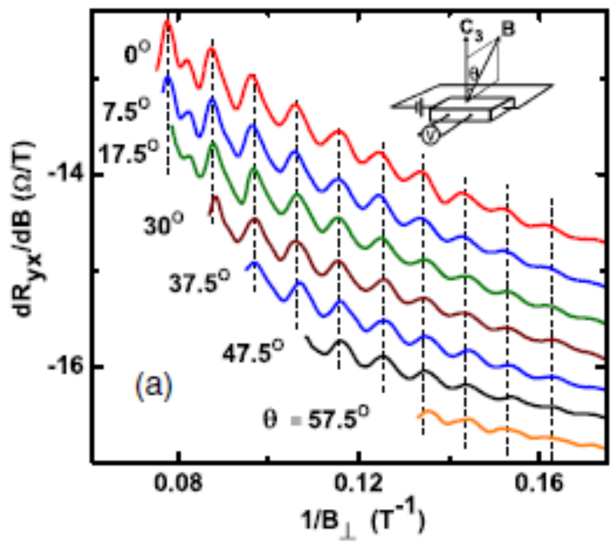

Weak-anti localization

Bi_2Se_3 thin film

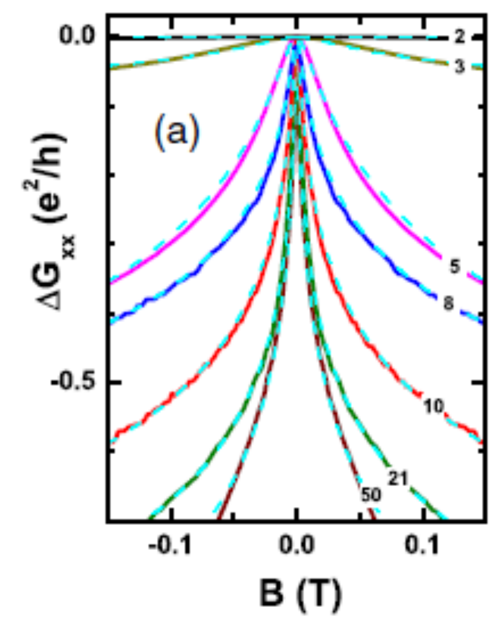

A. A. Taskin et al., Phys. Rev. Lett. **109**, 066803 (2012).

Detection of spin accumulation in topological insulator

nature nanotechnology ARTICLES
PUBLISHED ONLINE: 23 FEBRUARY 2014 | DOI: 10.1038/NNANO.2014.16

Electrical detection of charge-current-induced spin polarization due to spin-momentum locking in Bi_2Se_3

C. H. Li[1]*, O. M. J. van 't Erve[1], J. T. Robinson[2], Y. Liu[3], L. Li[3] and B. T. Jonker[1]*

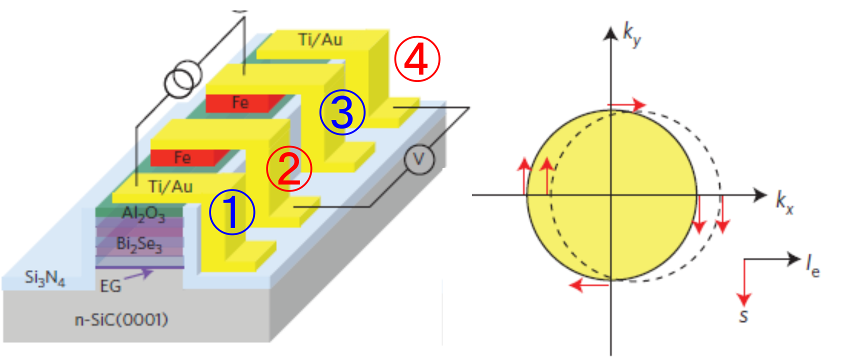

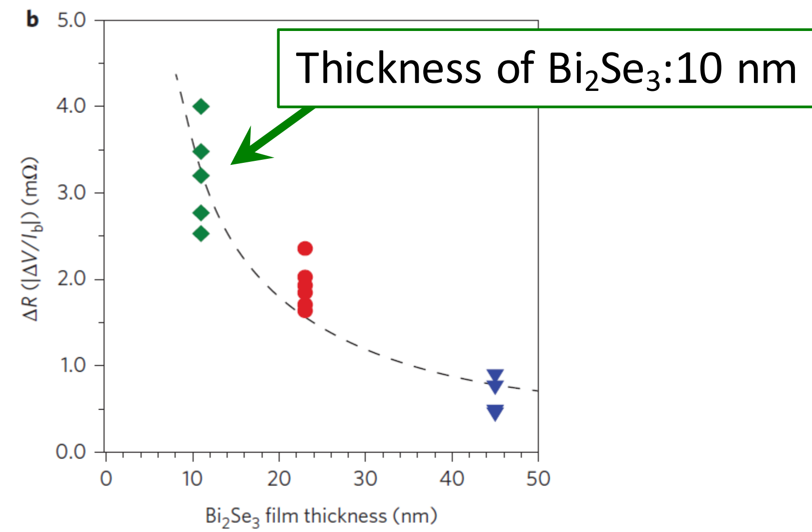

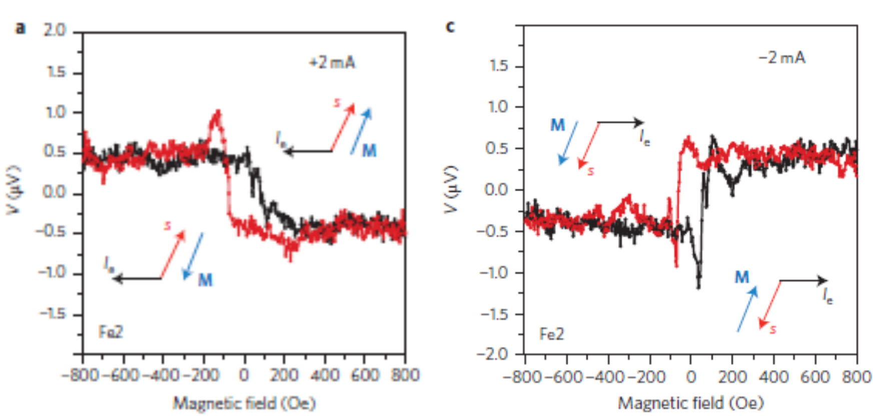

This study

- ✓ Bulk-insulating TI
- ✓ Extraction of spin current by electric fields. (Local magnetoresistance)

Magnetoresistance using nonlocal three-terminal scheme

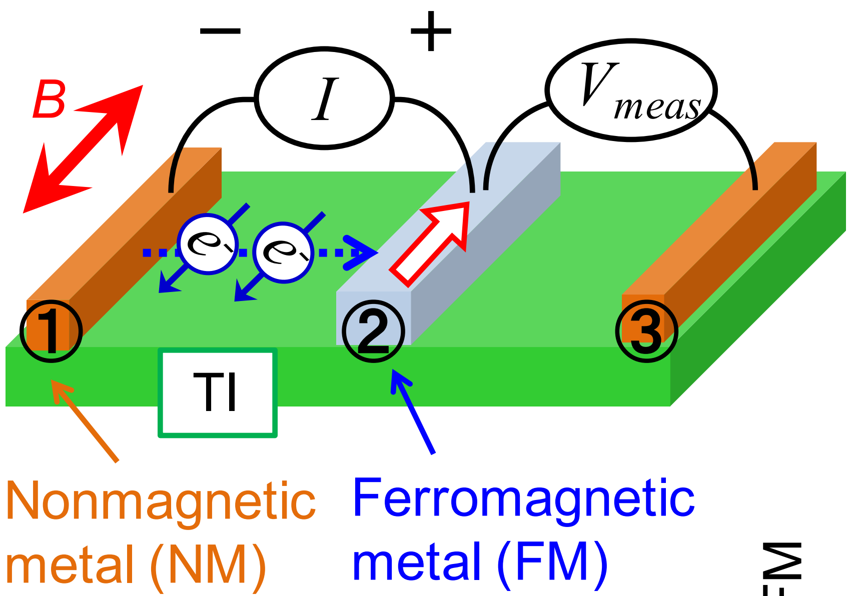

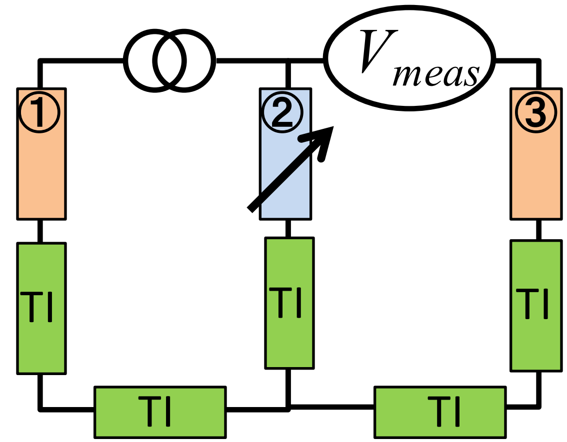

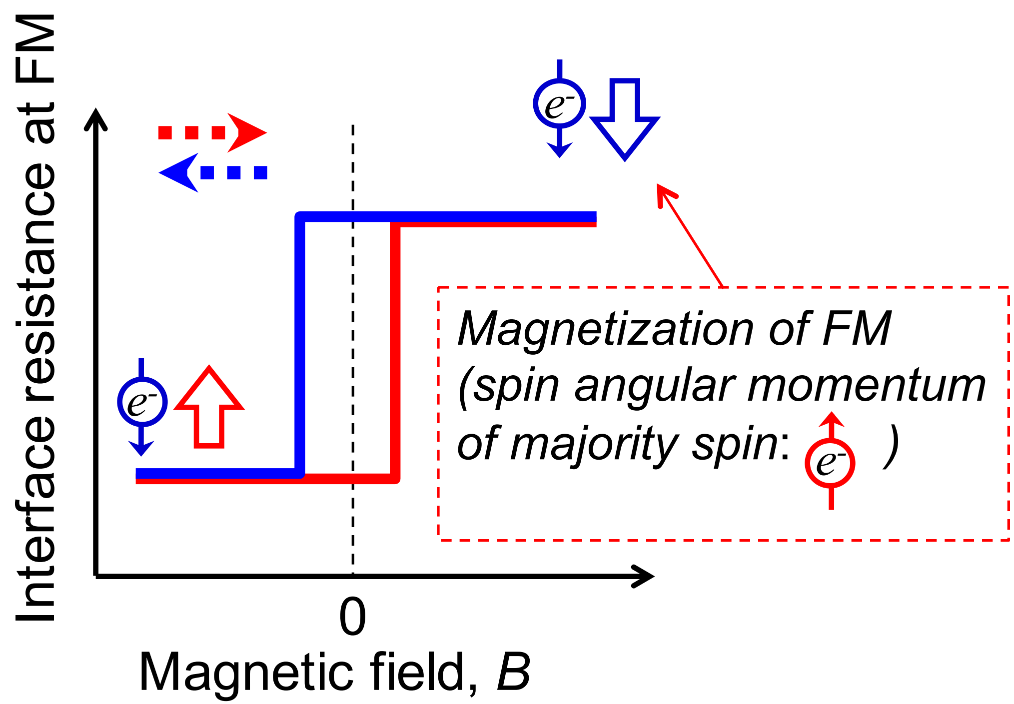

Magnetoresistance using nonlocal three-terminal scheme

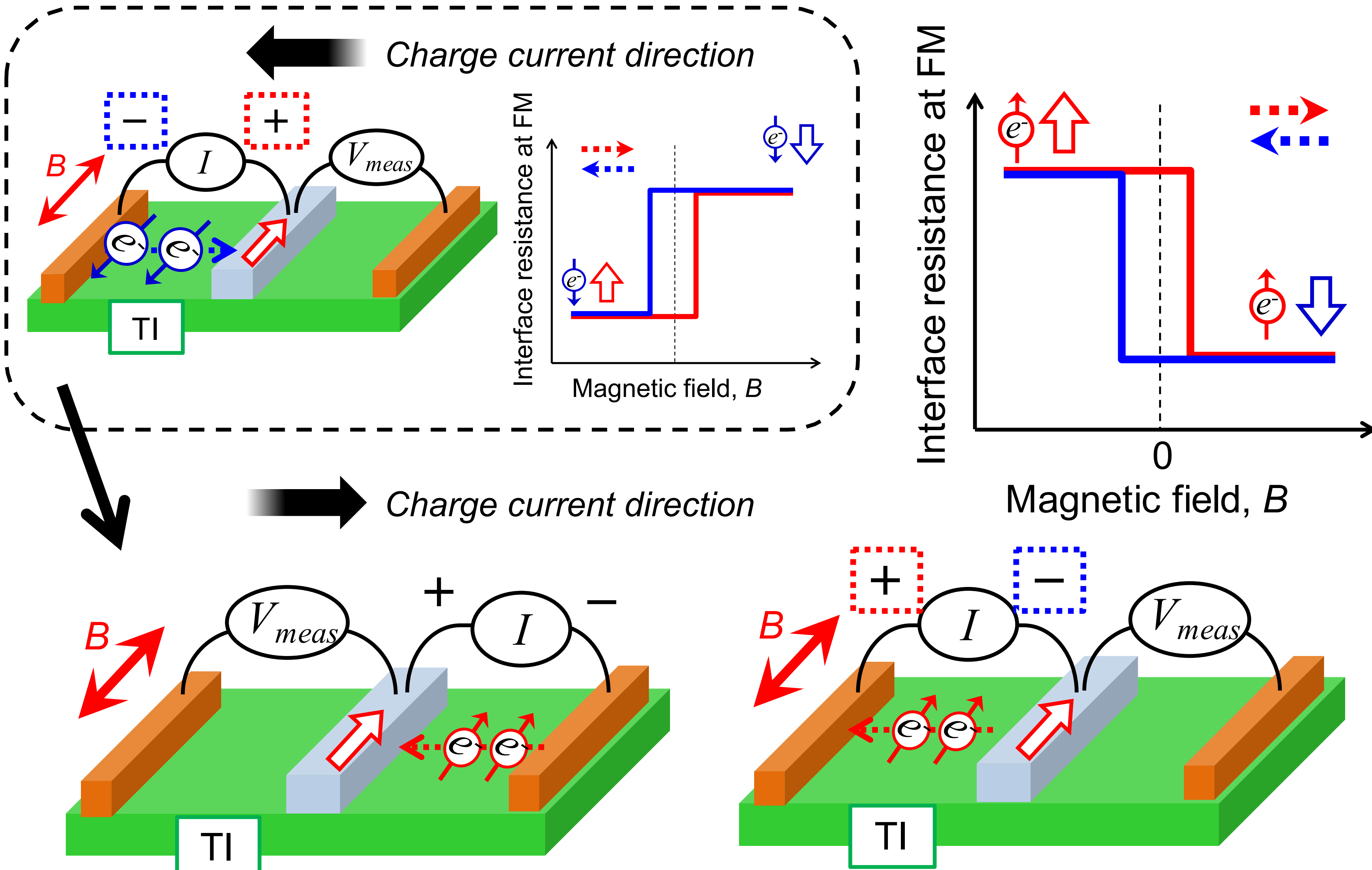

Change of current-voltage configuration

Change of current direction

Device fabrication procedure

Sample : Single crystal $Bi_{1.5}Sb_{0.5}Te_{1.7}Se_{1.3}$ (BSTS) & Bi_2Se_3 formed by a Bridgeman method

Substrate : Thermally-oxidized SiO_2 (500 nm) / Si

TI flakes : Mechanical exfoliation using a Scotch tape

Thickness of TI-flake : Laser microscope& Atomic force microscope.

$Ni_{80}Fe_{20}$(Py) & Au/Cr electrode : Electron beam lithography & Electron beam evaporation.

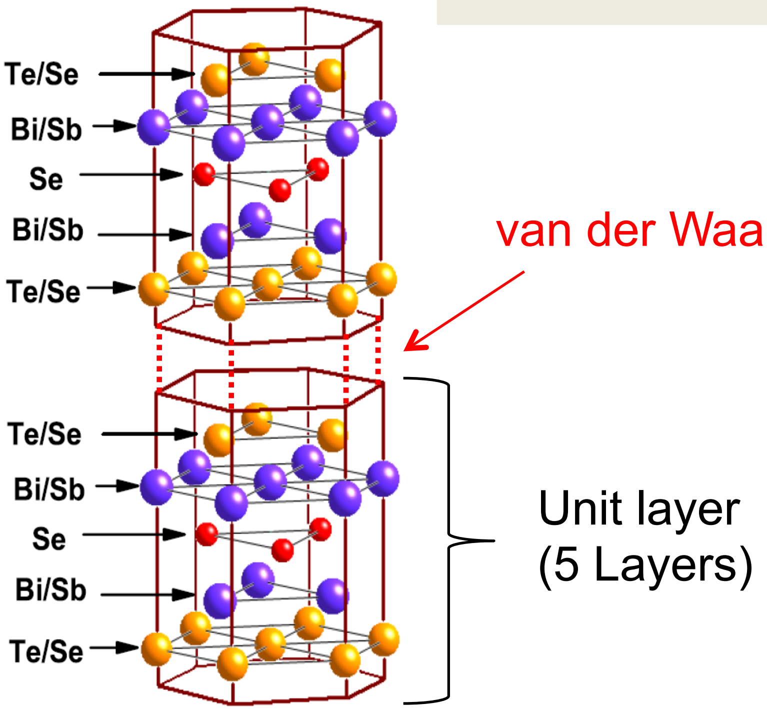

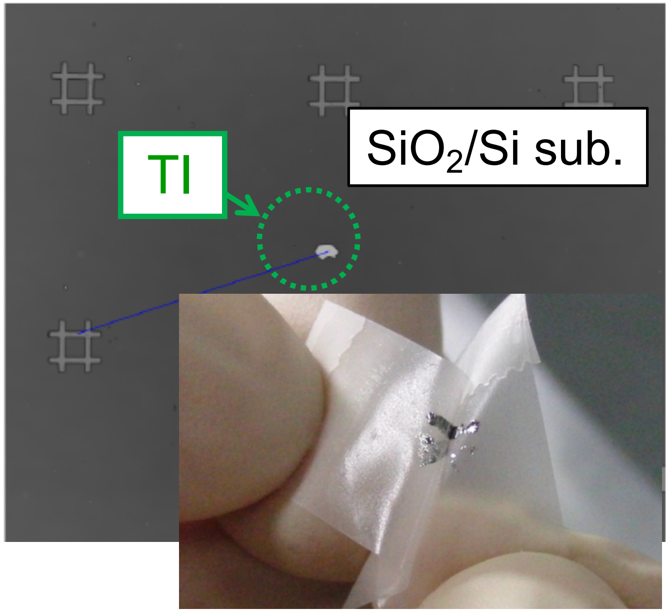

A. A. Taskin et al., Phys. Rev. Lett. **107**, 016801 (2011).

Device fabrication procedure

Sample : Single crystal $Bi_{1.5}Sb_{0.5}Te_{1.7}Se_{1.3}$ (BSTS) & Bi_2Se_3 formed by a Bridgeman method

Substrate : Thermally-oxidized SiO_2 (500 nm) / Si

TI flakes : Mechanical exfoliation using a Scotch tape

Thickness of TI-flake : Laser microscope& Atomic force microscope.

$Ni_{80}Fe_{20}$(Py) & Au/Cr electrode : Electron beam lithography & Electron beam evaporation.

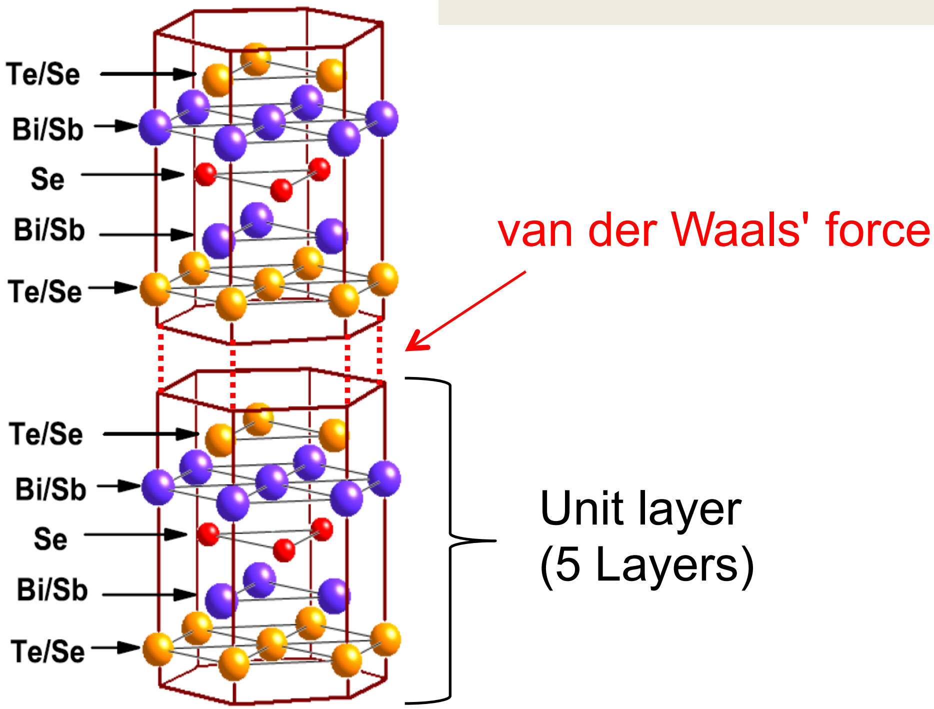

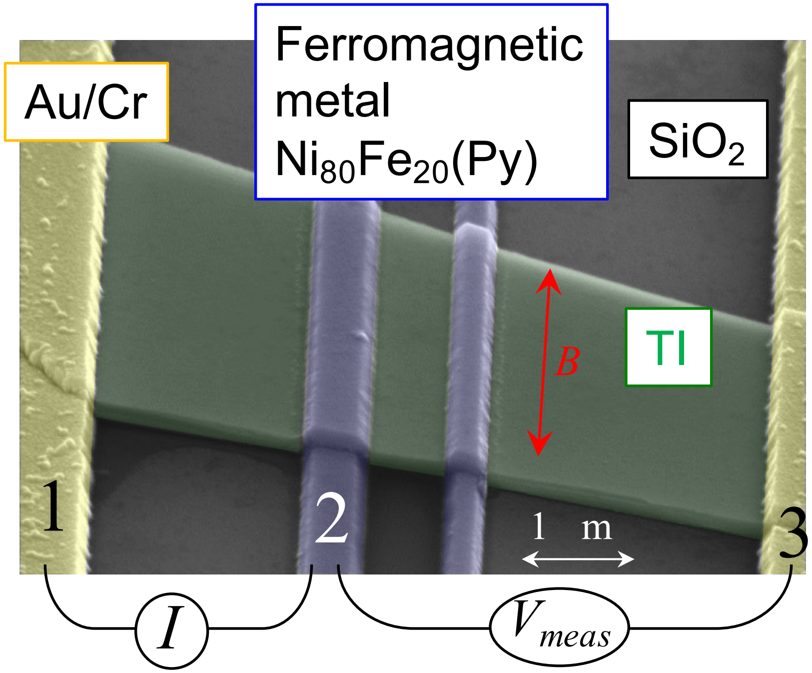

A. A. Taskin et al., Phys. Rev. Lett. **107**, 016801 (2011).

Temperature dependence of resistivity

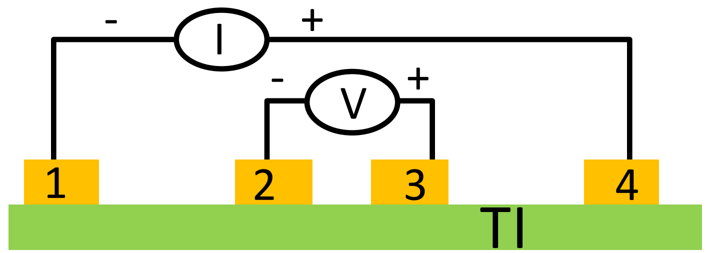

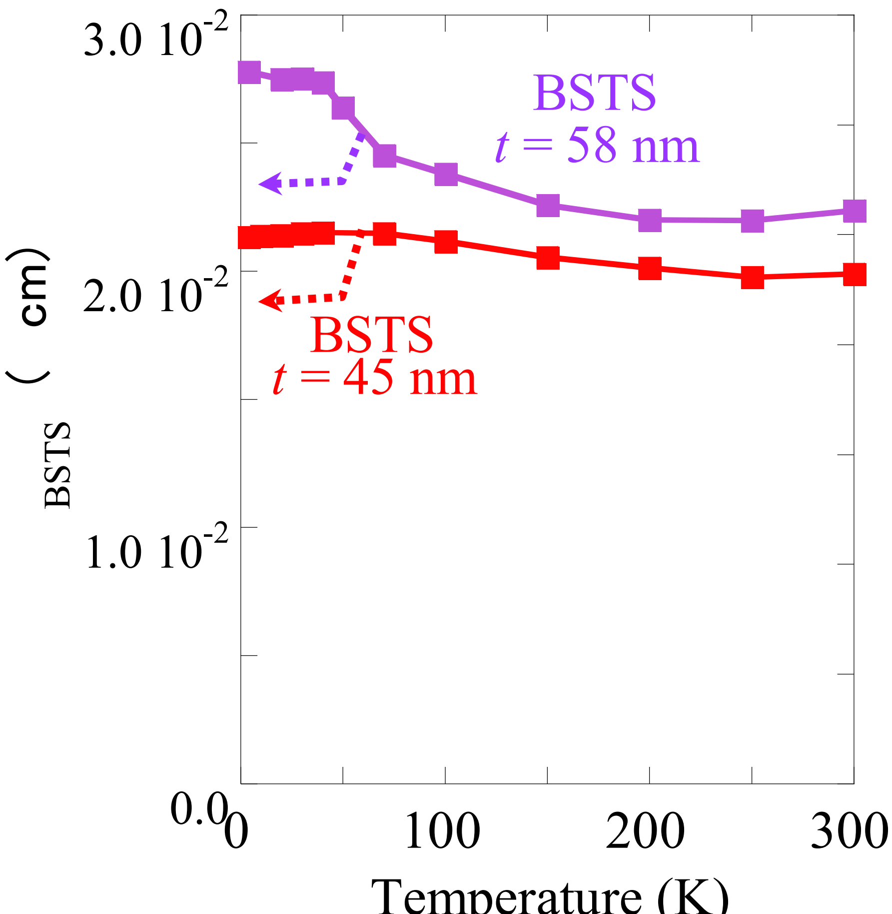

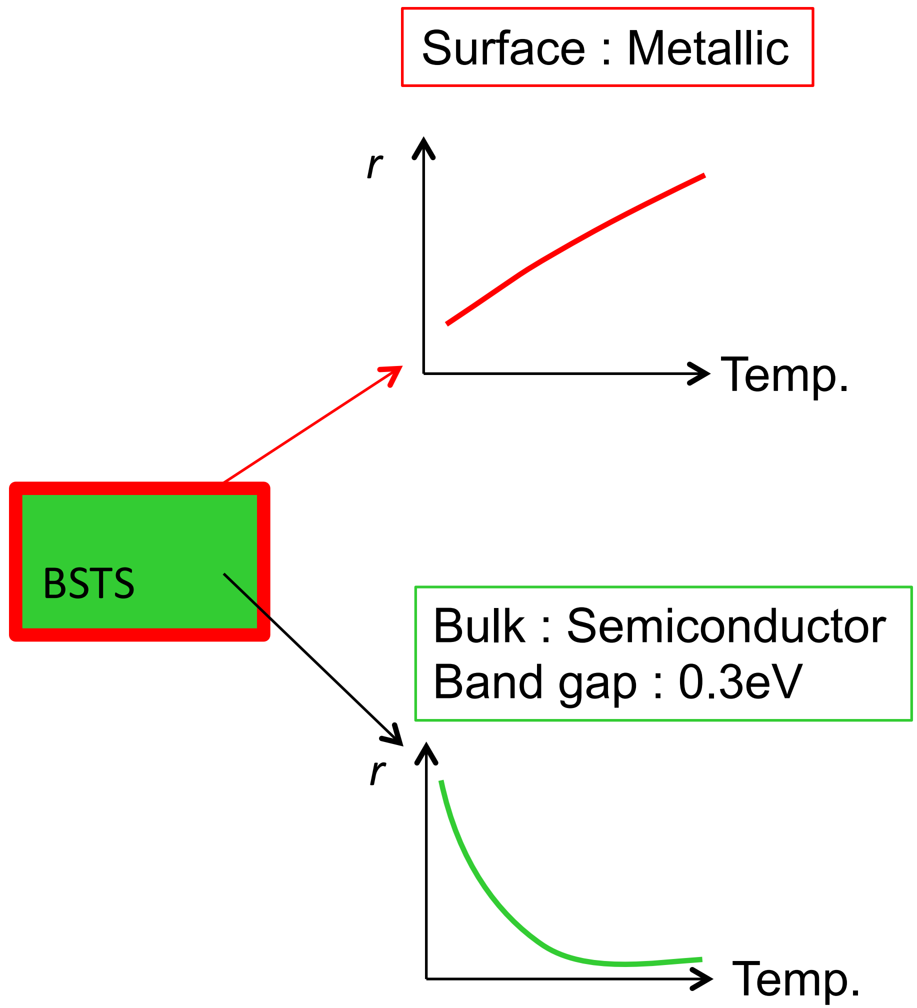

Temperature dependence of resistivity

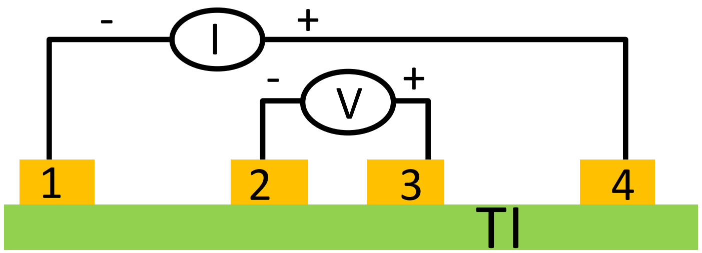

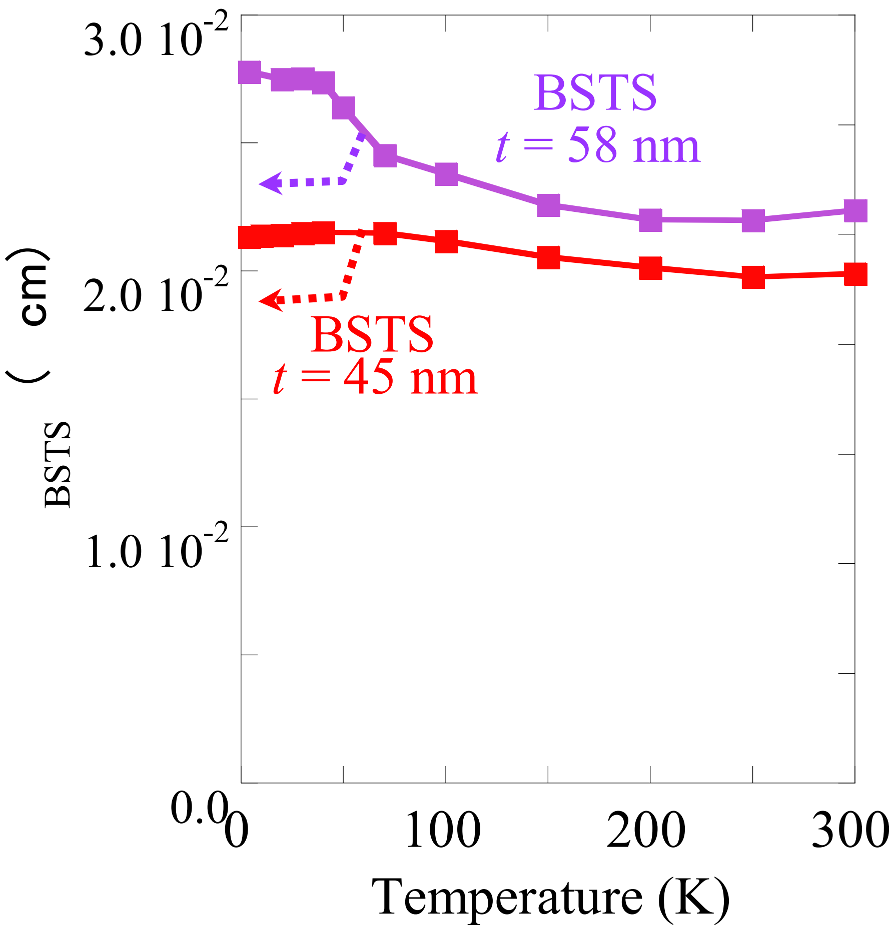

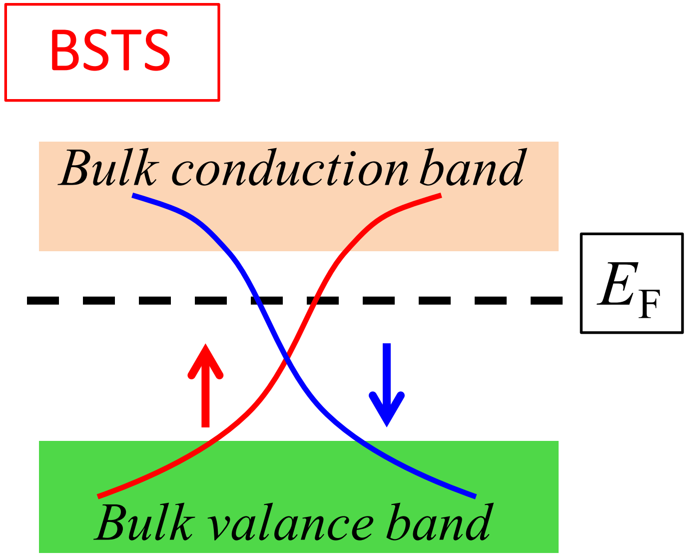

Temperature dependence of resistivity

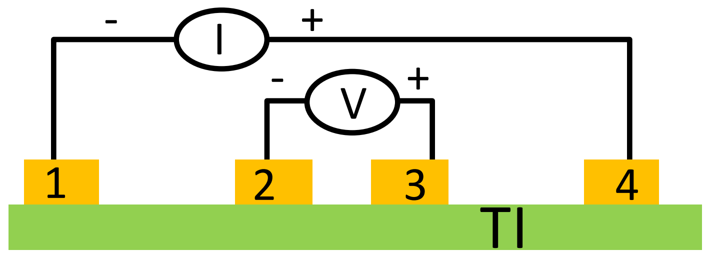

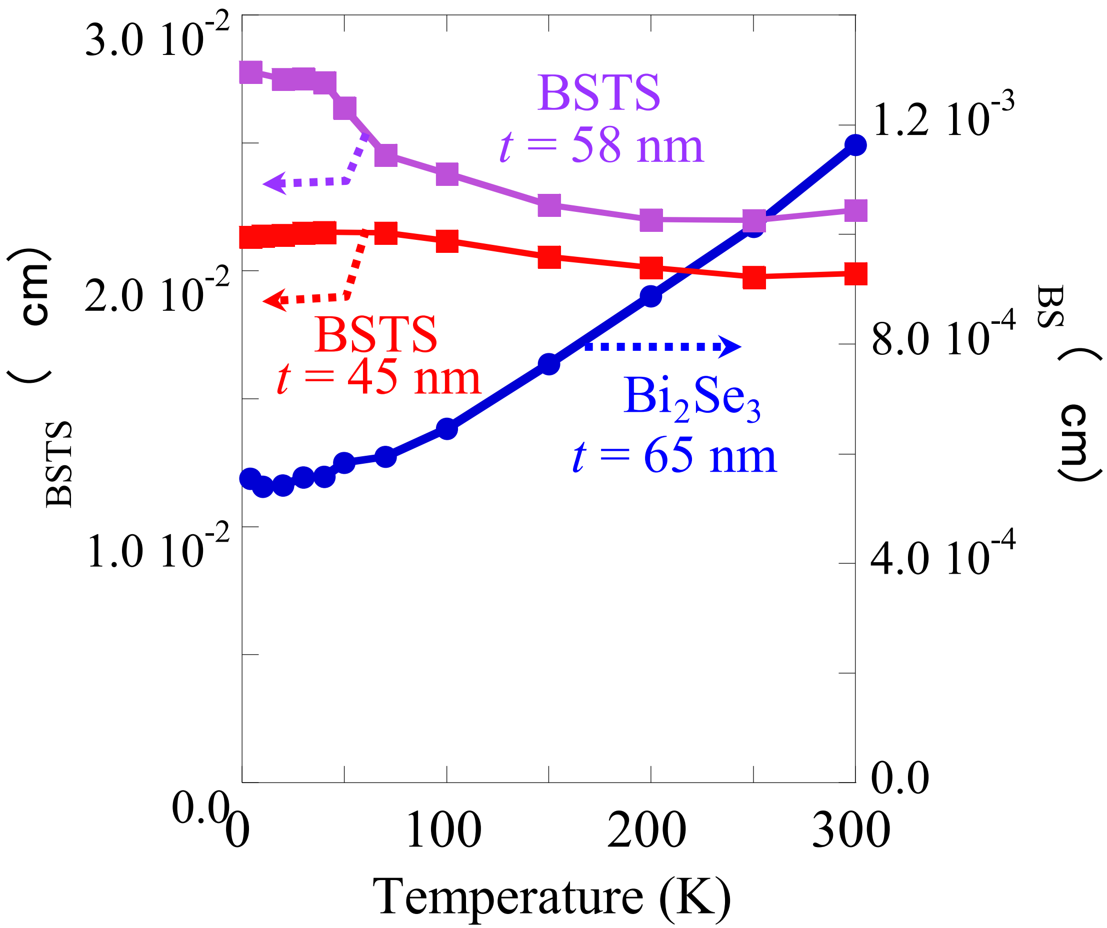

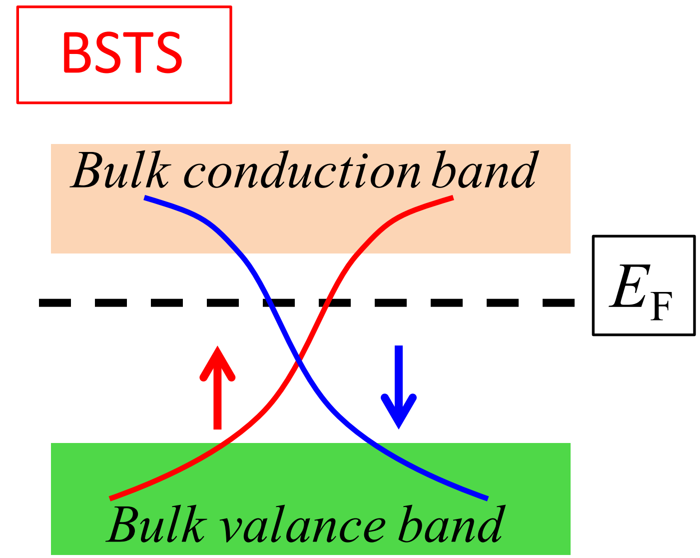

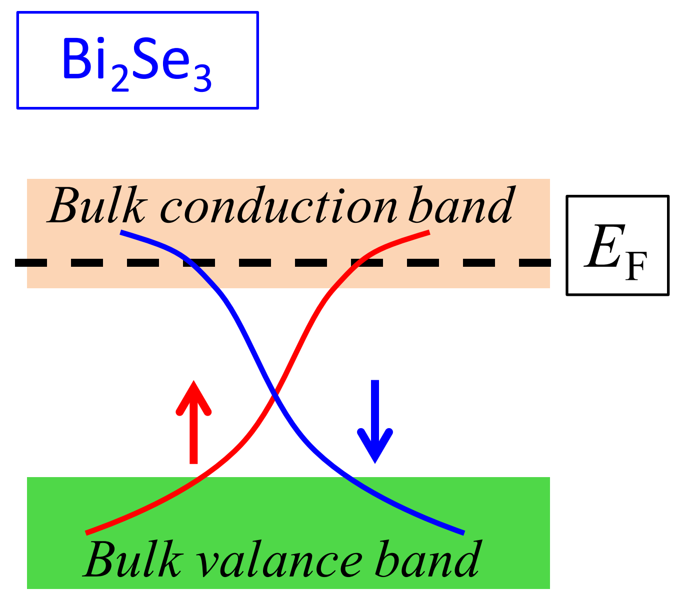

Magnetoresistance in BSTS devices at 4.2 K

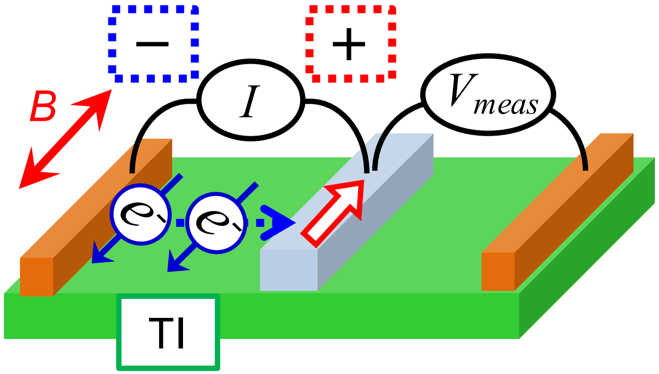

4.2 K

I =100 mA

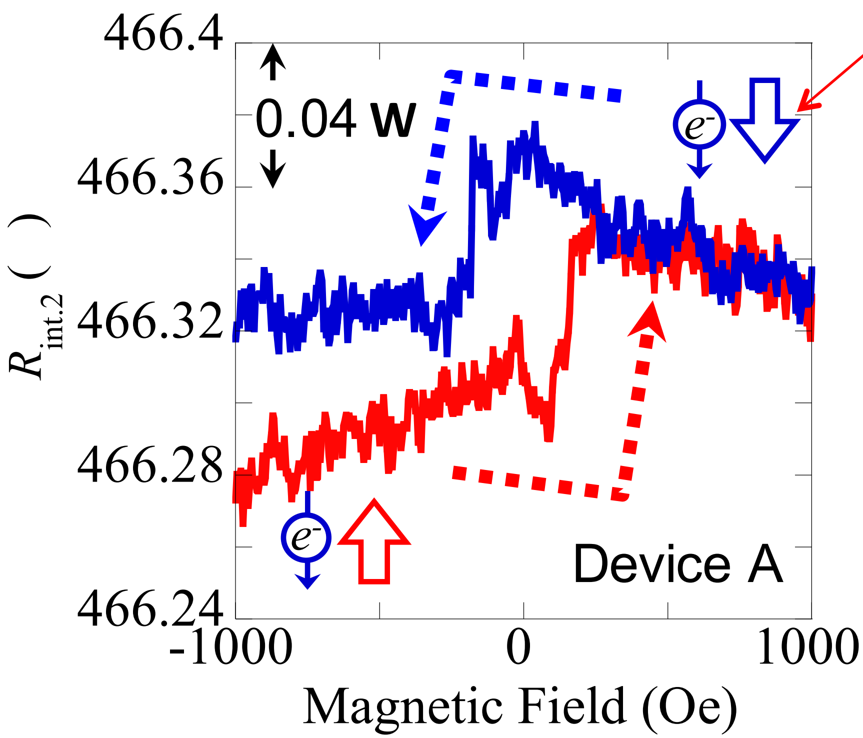

Magnetization of FM
(Spin angular momentum
of majority spin: e^- *)*

Magnetoresistance in BSTS devices at 4.2 K

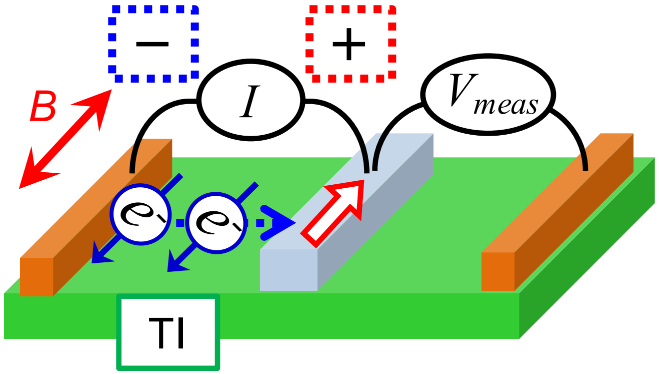

4.2 K

I =100 mA

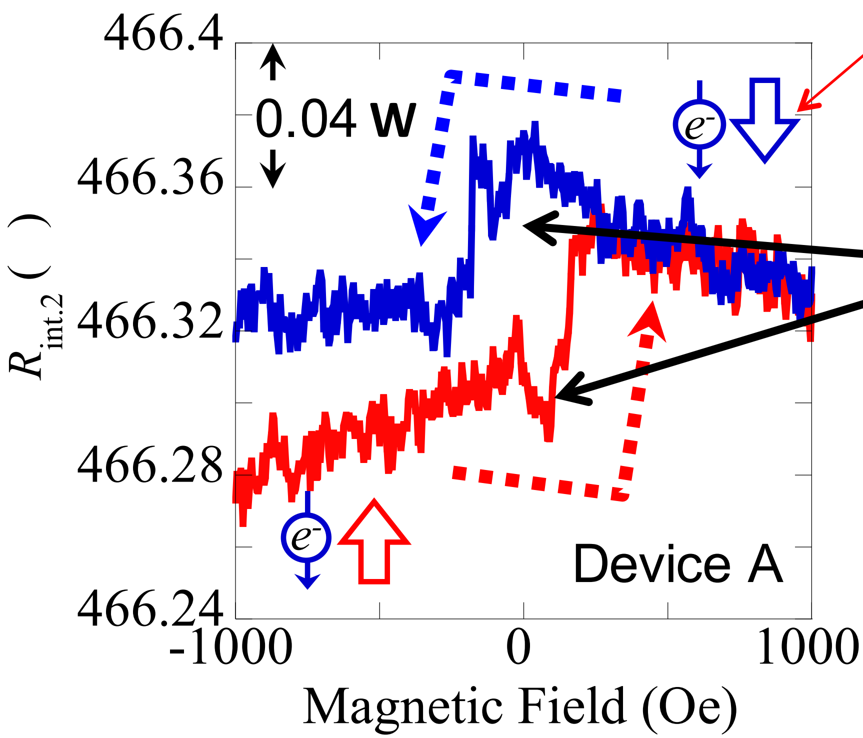

Magnetization of FM
(Spin angular momentum
of majority spin: e-)

Anisotropic magnetoresistance
(AMR)

Contact 2 : Py ⇒ Au/Py
Suppression of the Dip signals

Magnetoresistance in BSTS devices at 4.2 K

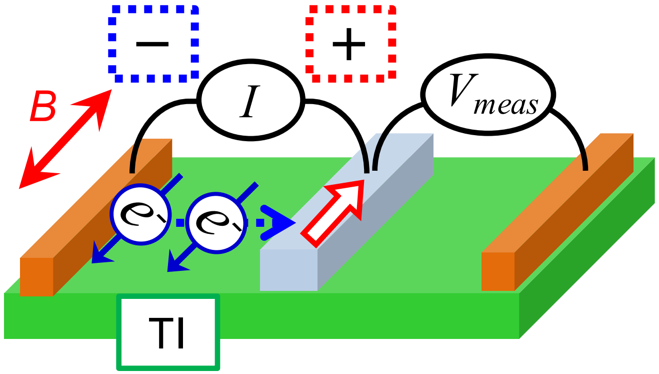

4.2 K

I =100 mA

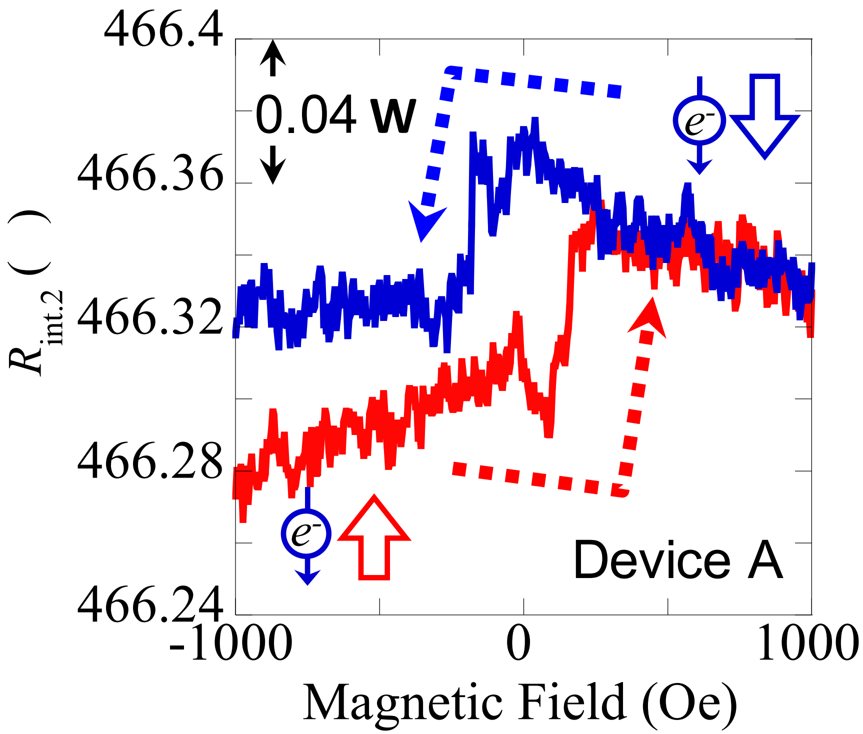

I =-100 mA

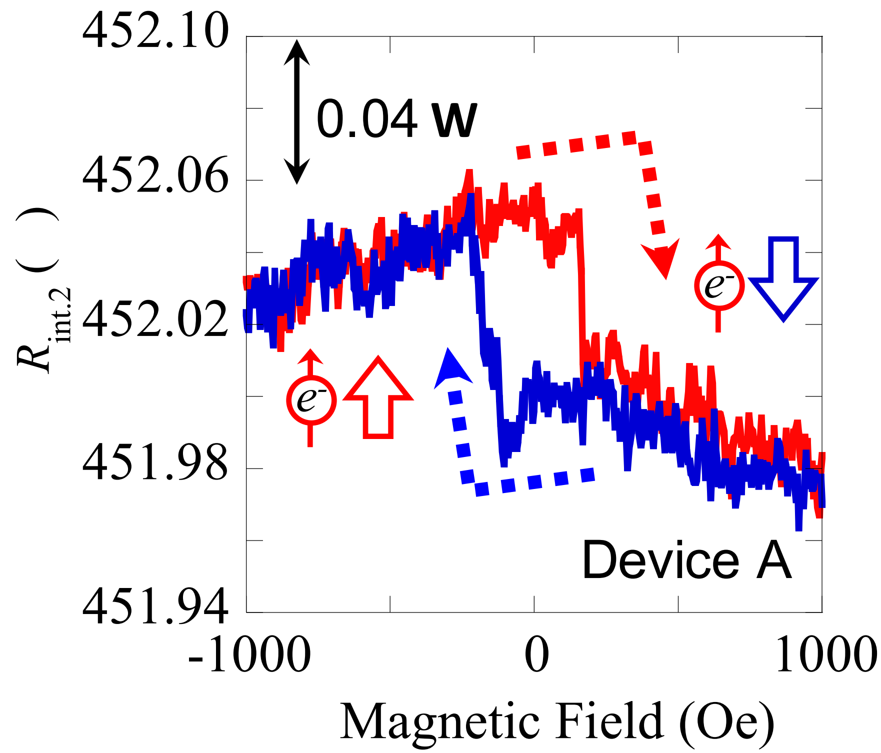

Reversal of the current-voltage scheme

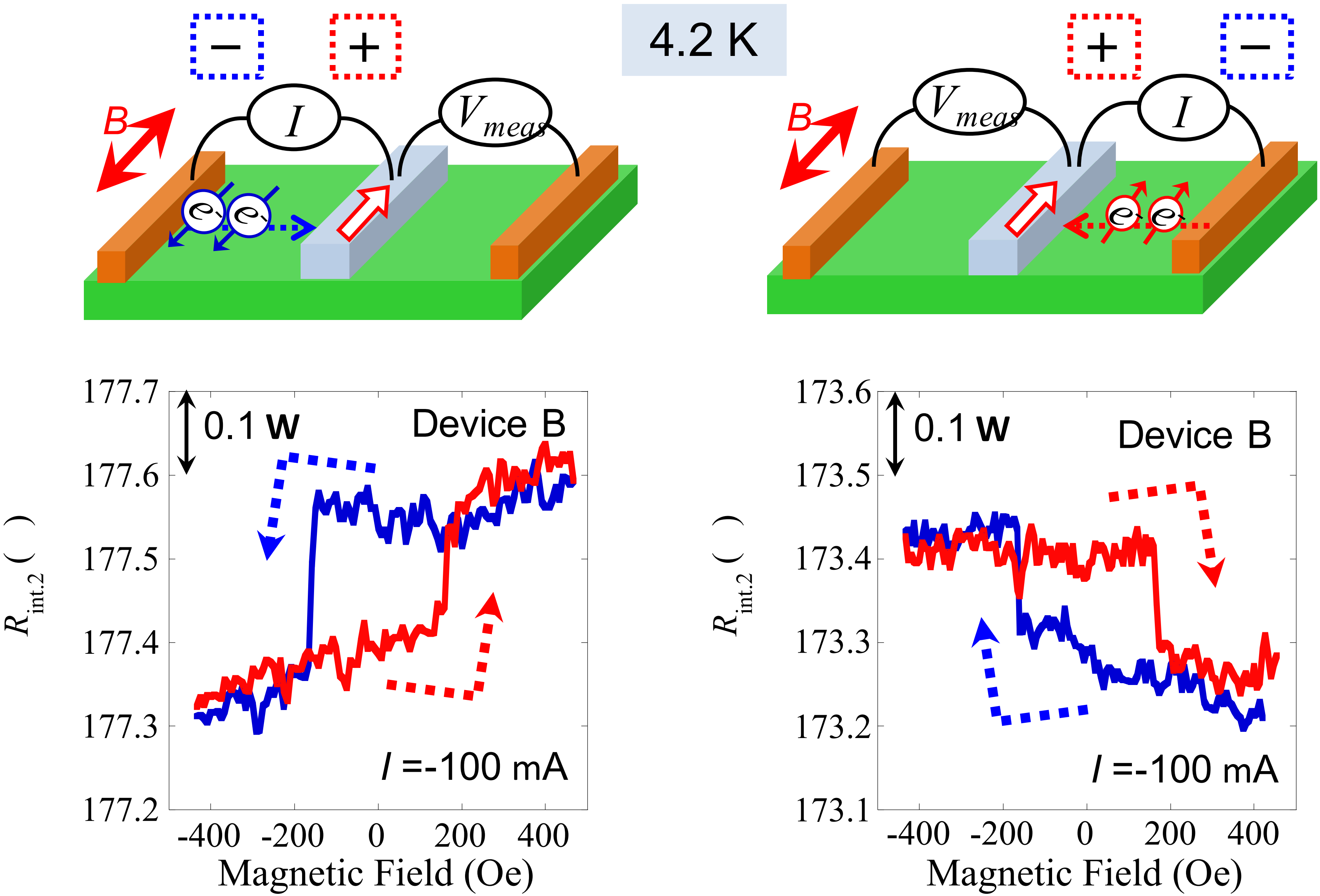

Magnetoresistance at *B* // *I*

4.2 K

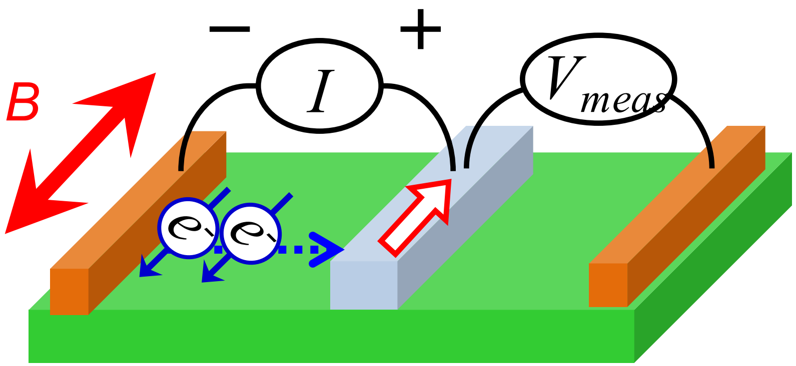

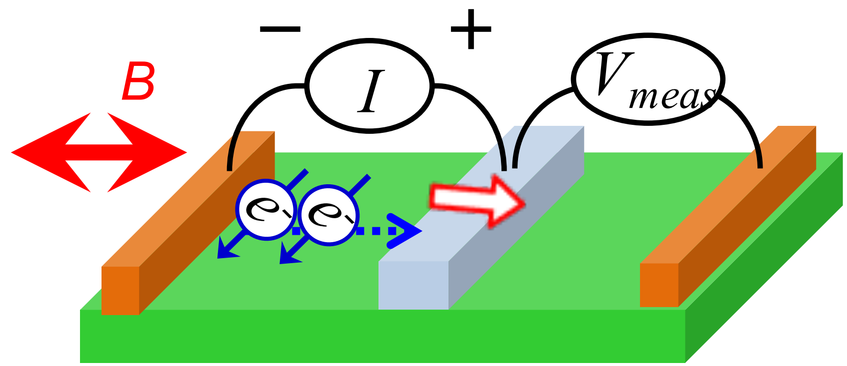

Device D

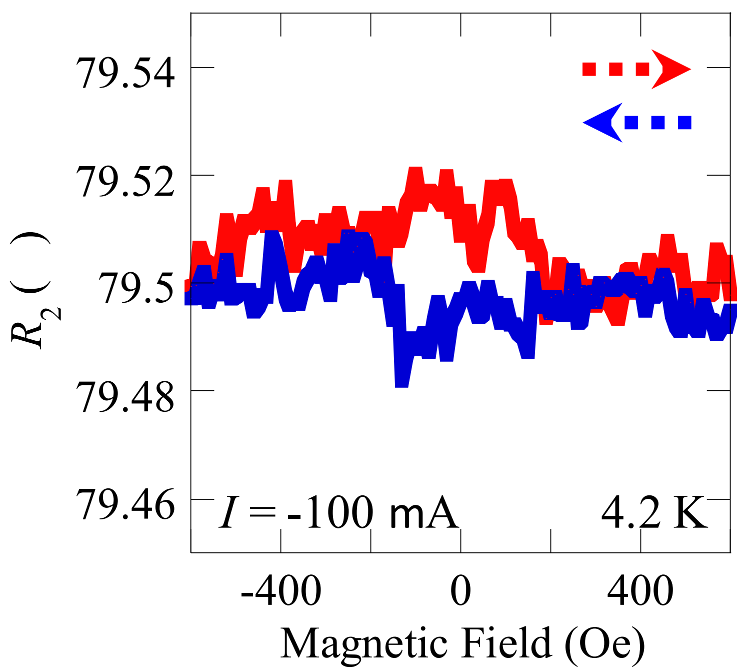

Device D

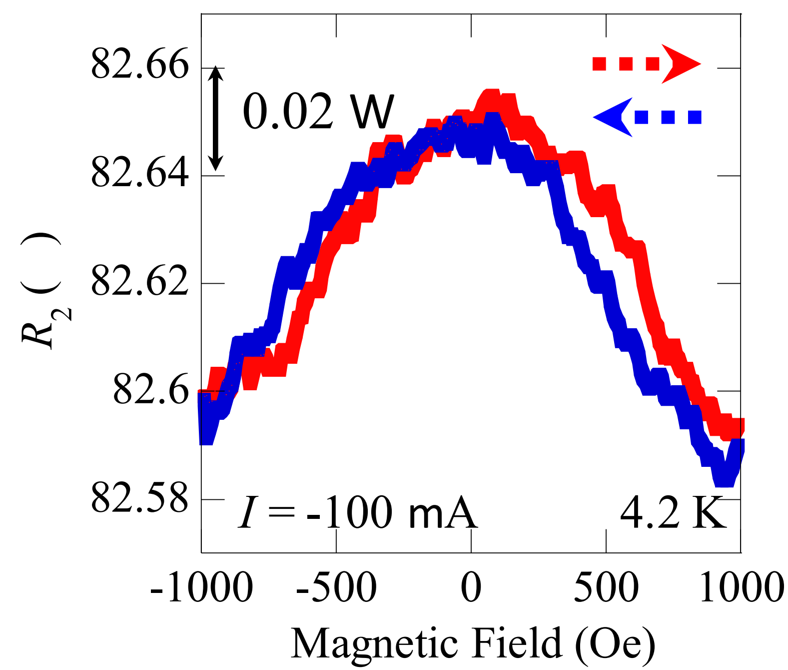

Magnetoresistance in Bi_2Se_3 devices

4.2 K

I =100 mA

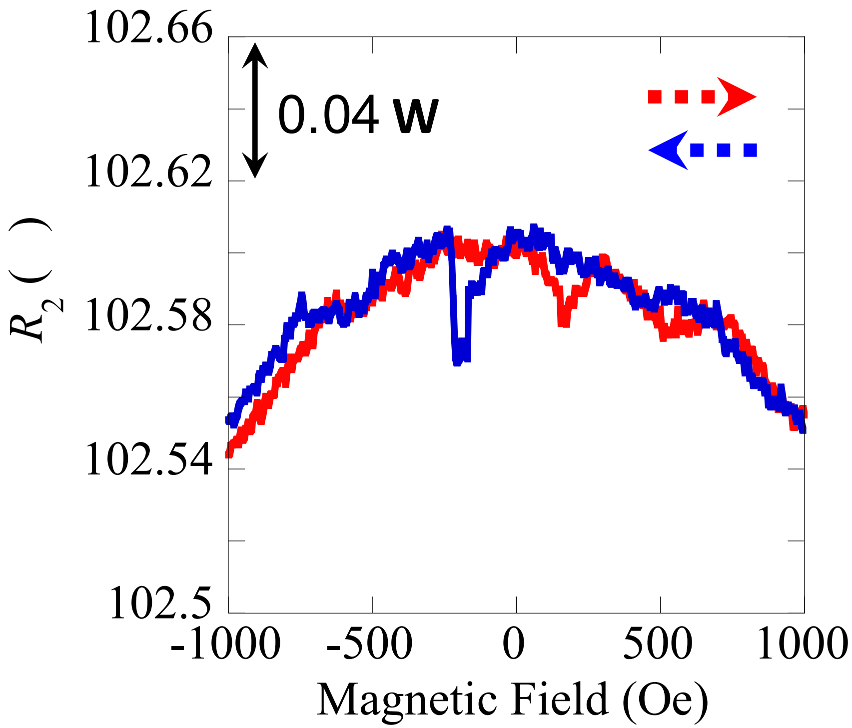

I =-100 mA

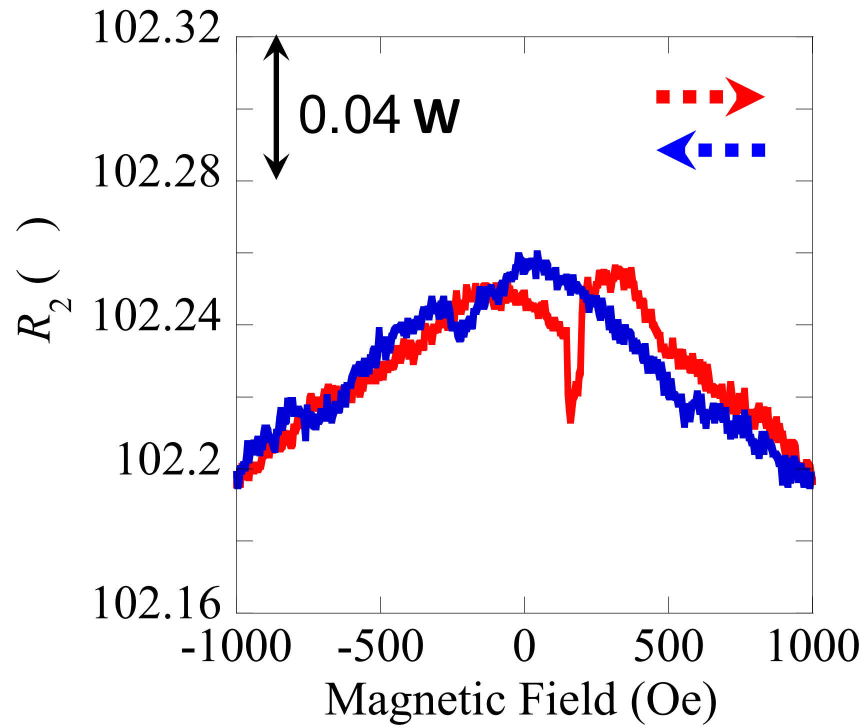

No rectangular hysteresis signals

Estimation of charge current density in the surface state

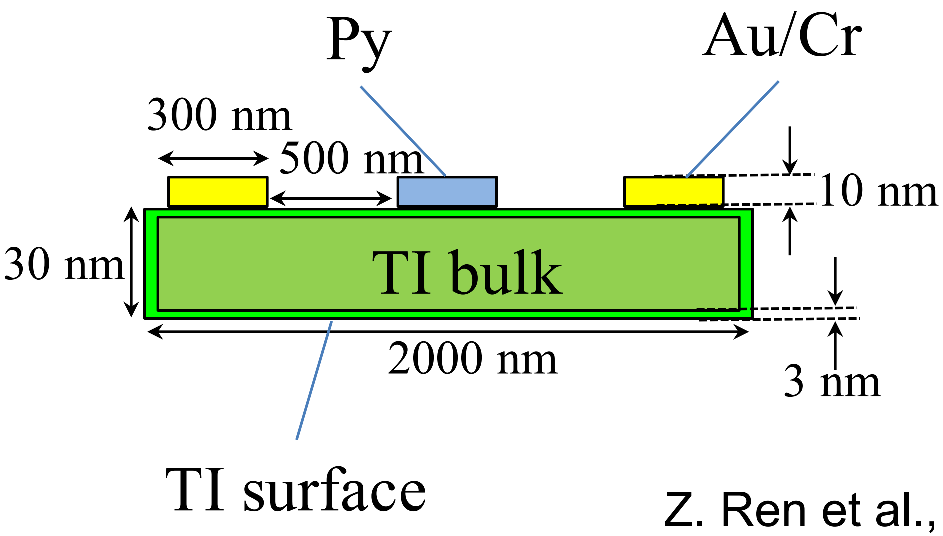

s_{Py}=2.50 × 10^{0} $W^{-1}mm^{-1}$
$s_{BS\ surface}$=2.13 × 10^{0} $W^{-1}mm^{-1}$
$s_{BSTS\ surface}$=2.32 × 10^{-2} $W^{-1}mm^{-1}$
$s_{BS\ bulk}$=2.72 × 10^{-1} $W^{-1}mm^{-1}$
$s_{BSTS\ bulk}$=2.10 × 10^{-5} $W^{-1}mm^{-1}$

Z. Ren et al., Phys. Rev. B **84**, 165311(2011).
H. Steinberg et al., Nano Lett. **10**, 5032(2010).

Estimation of charge current density in the surface state

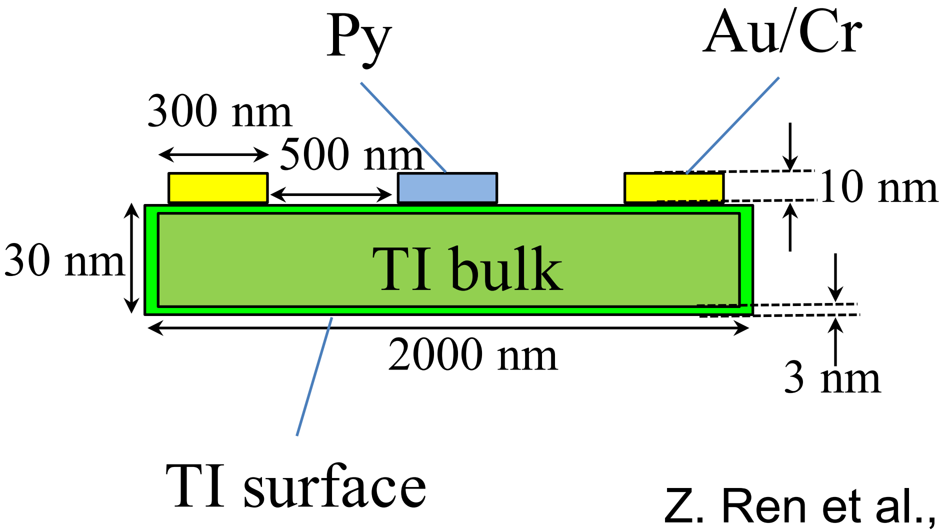

$s_{Py}=2.50\times10^{0}\ W^{-1}mm^{-1}$

$s_{BS\ surface}=2.13\times10^{0}\ W^{-1}mm^{-1}$

$s_{BSTS\ surface}=2.32\times10^{-2}\ W^{-1}mm^{-1}$

$s_{BS\ bulk}=2.72\times10^{-1}\ W^{-1}mm^{-1}$

$s_{BSTS\ bulk}=2.10\times10^{-5}\ W^{-1}mm^{-1}$

Z. Ren et al., Phys. Rev. B **84**, 165311(2011).
H. Steinberg et al., Nano Lett. **10**, 5032(2010).

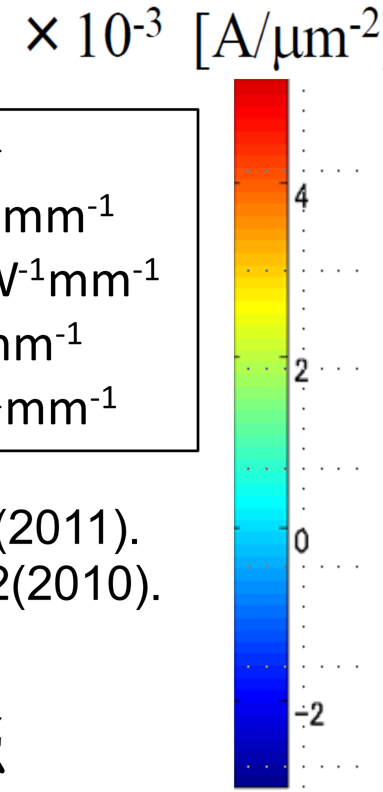

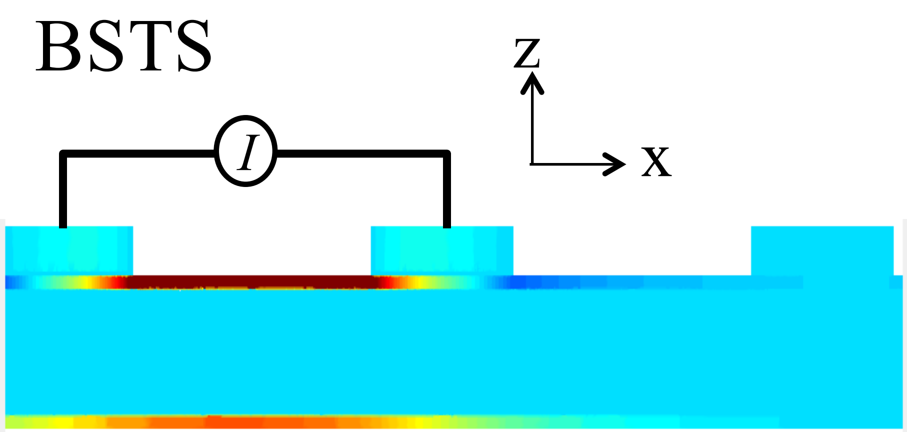

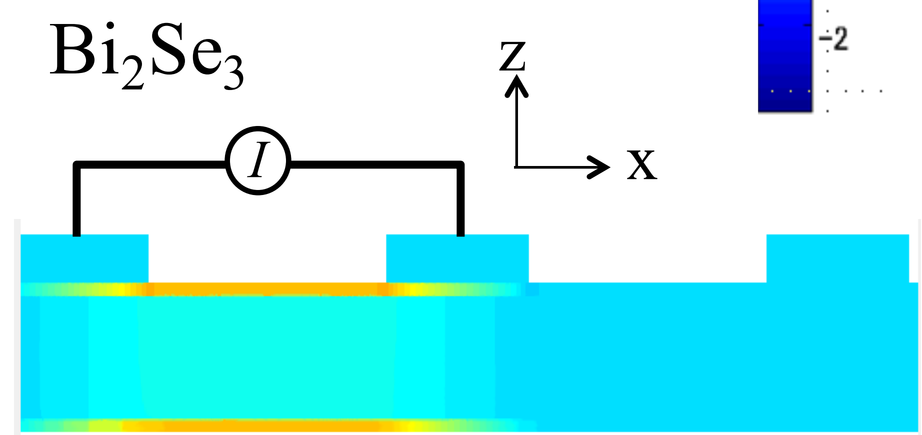

Estimation of charge current density in the surface state

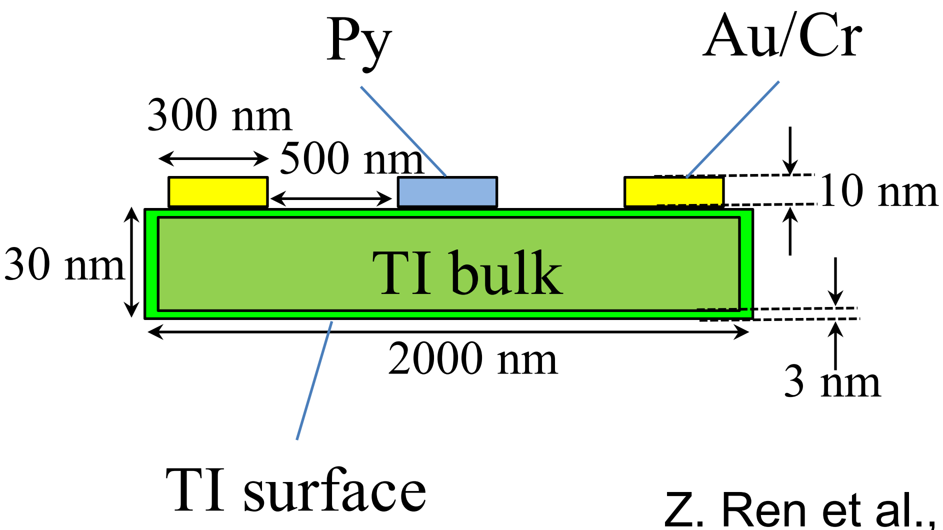

s_{Py}=2.50 × 10^{0} W^{-1}mm^{-1}

$s_{BS\ surface}$=2.13 × 10^{0} W^{-1}mm^{-1}

$s_{BSTS\ surface}$=2.32 × 10^{-2} W^{-1}mm^{-1}

$s_{BS\ bulk}$=2.72 × 10^{-1} W^{-1}mm^{-1}

$s_{BSTS\ bulk}$=2.10 × 10^{-5} W^{-1}mm^{-1}

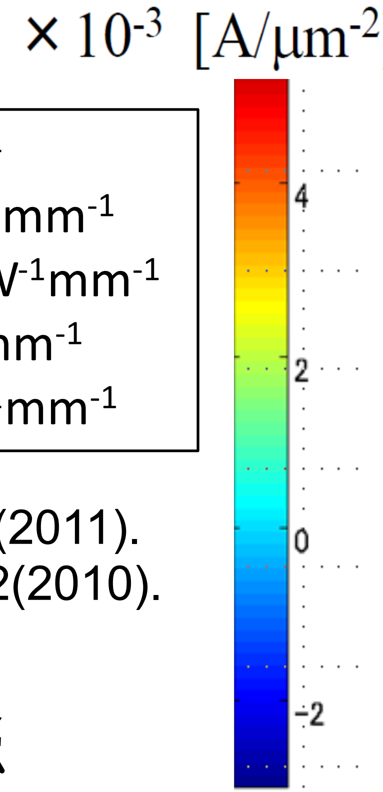

Z. Ren et al., Phys. Rev. B **84**, 165311(2011).
H. Steinberg et al., Nano Lett. **10**, 5032(2010).

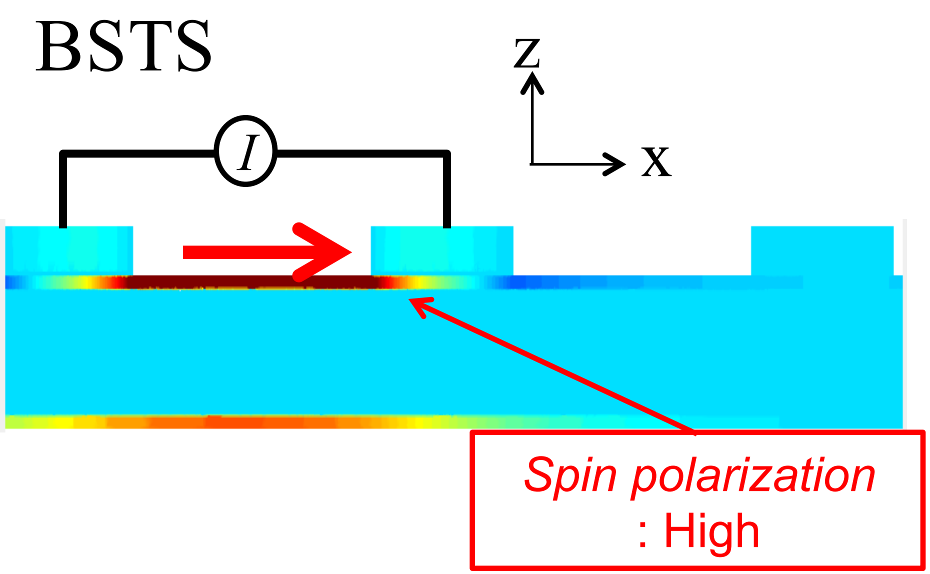

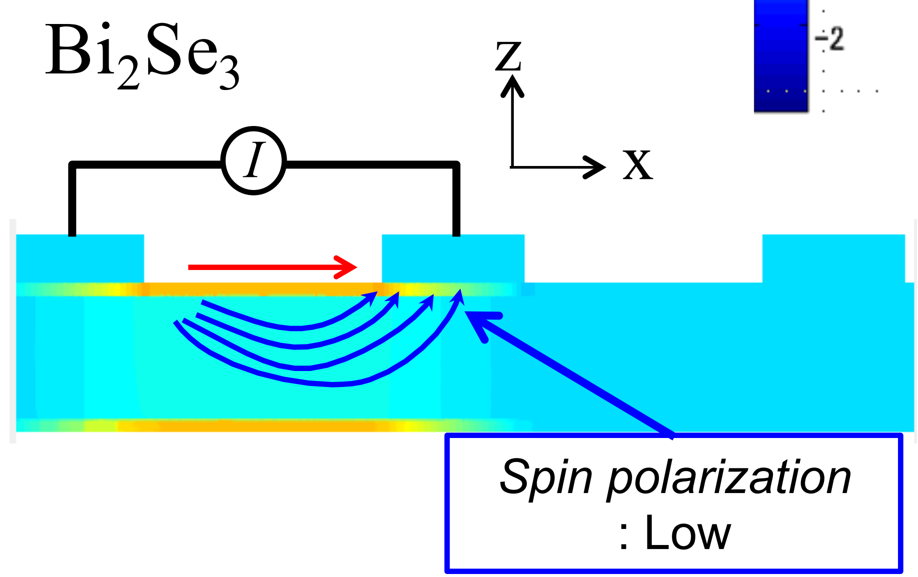

Magnetoresistance in BSTS devices at 300 K

300 K

I =100 mA

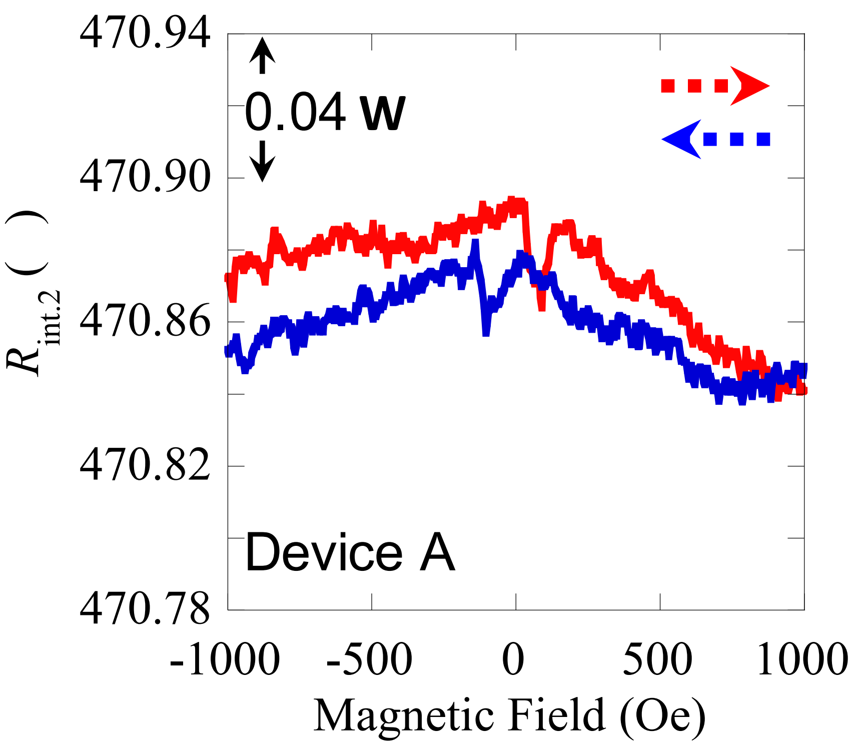

I =-100 mA

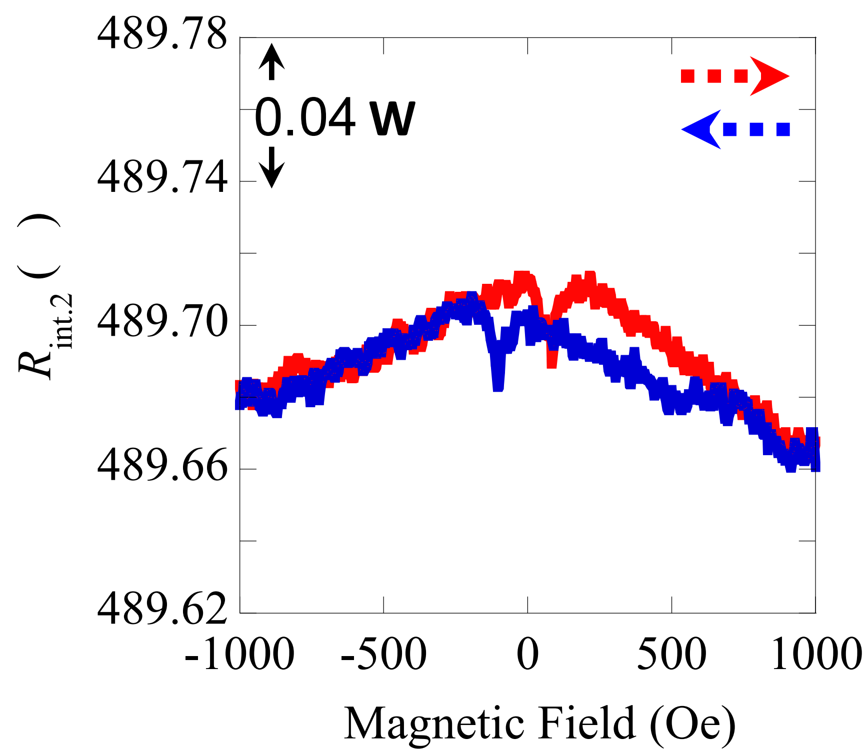

Rectangular hysteresis signals : Disappeared
AMR signals : Observed

Magnetoresistance in BSTS devices at 300 K

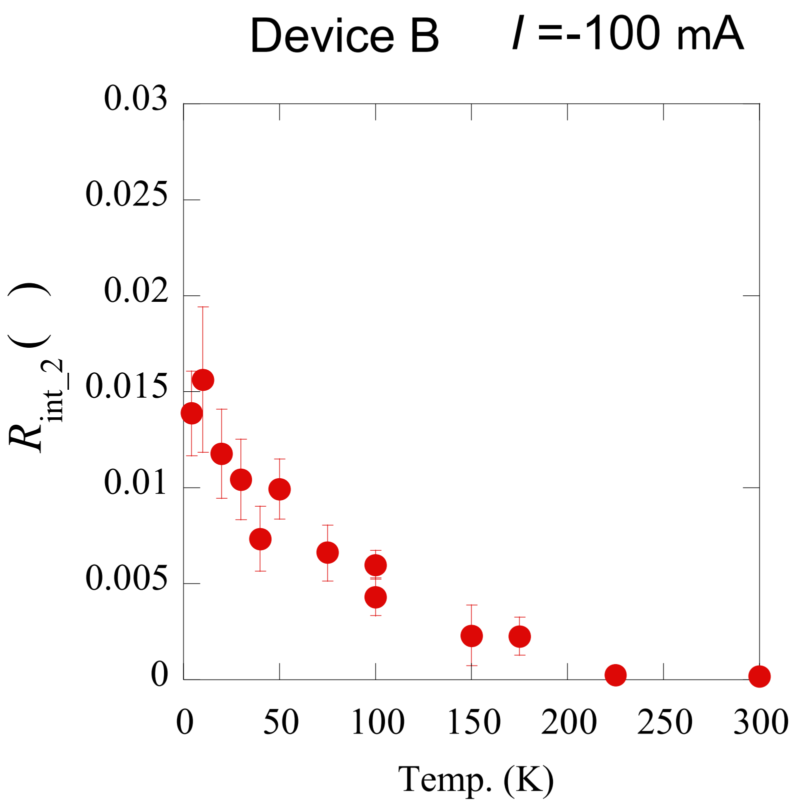

Disappearance of the rectangular signals : 150~200 K

Magnetoresistance in BSTS devices at 300 K

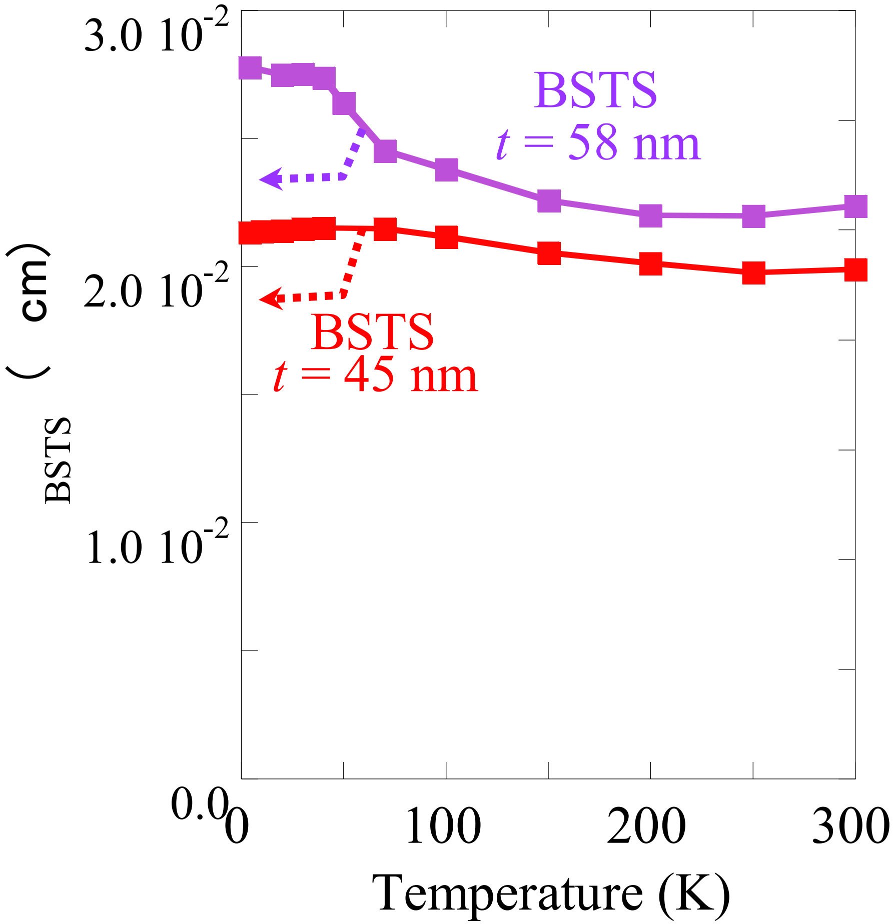

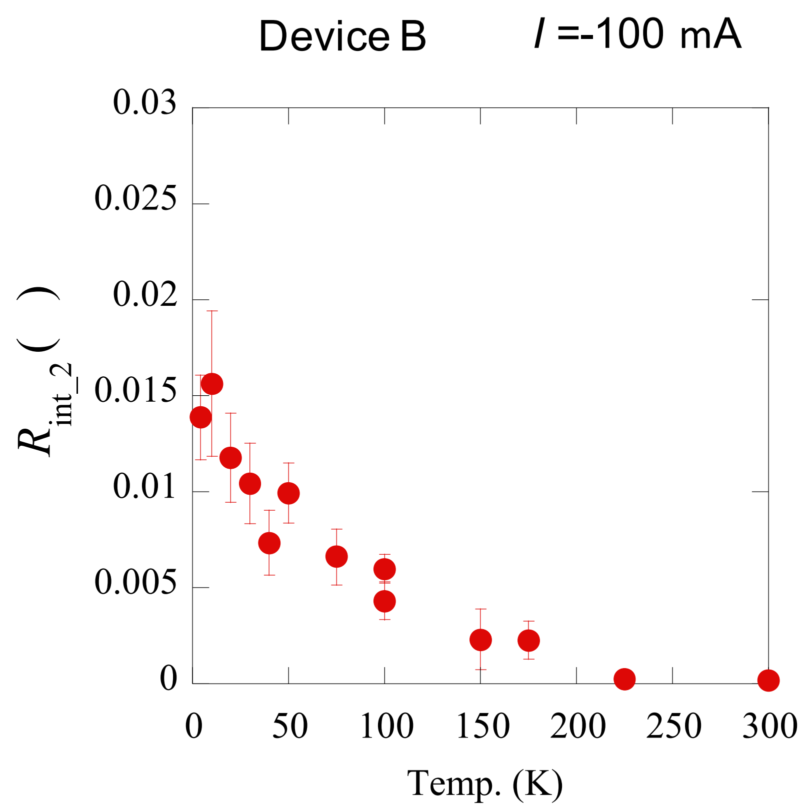

$$\frac{\rho_{BSTS}\ @4.2K}{\rho_{BSTS}\ @300K} = 1.07 \sim 1.43$$

⇒ Considerable surface conduction at 300 K.

Several mm thick BSTS

$$\frac{\rho_{BSTS}\ @8K}{\rho_{BSTS}\ @300K} = 10 \sim 100$$

Y. Ando JPSJ **82**, 102001 (2013).

Magnetoresistance in BSTS devices at 300 K

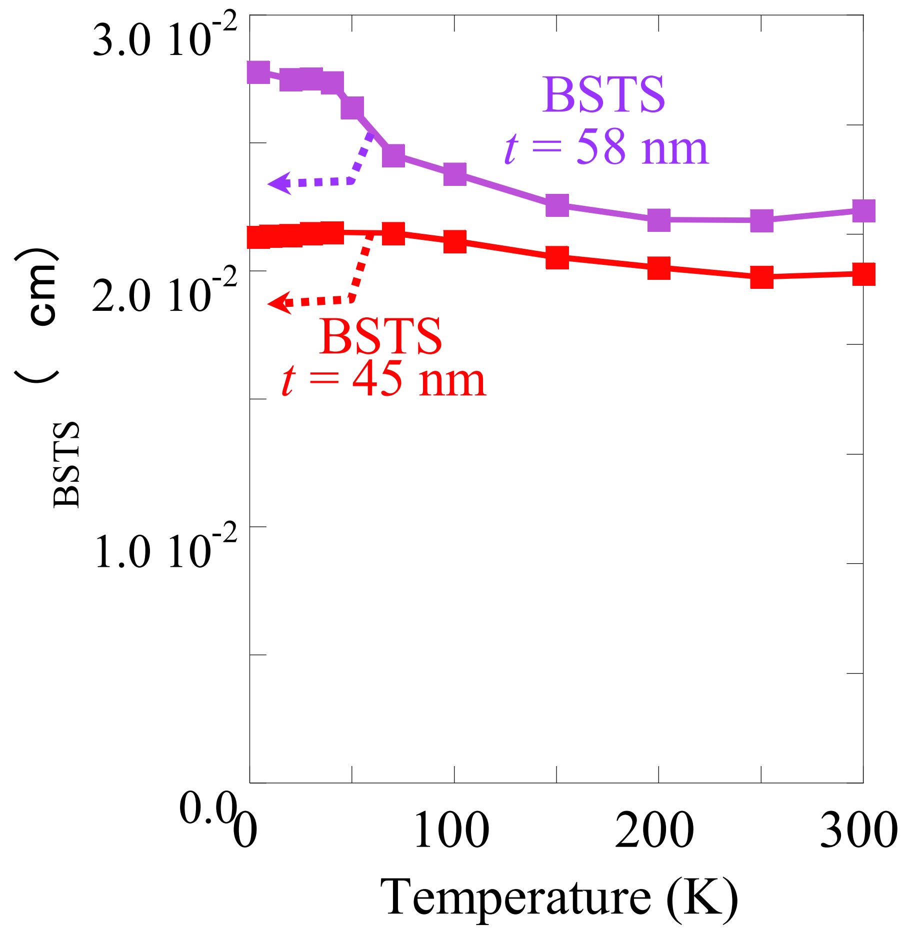

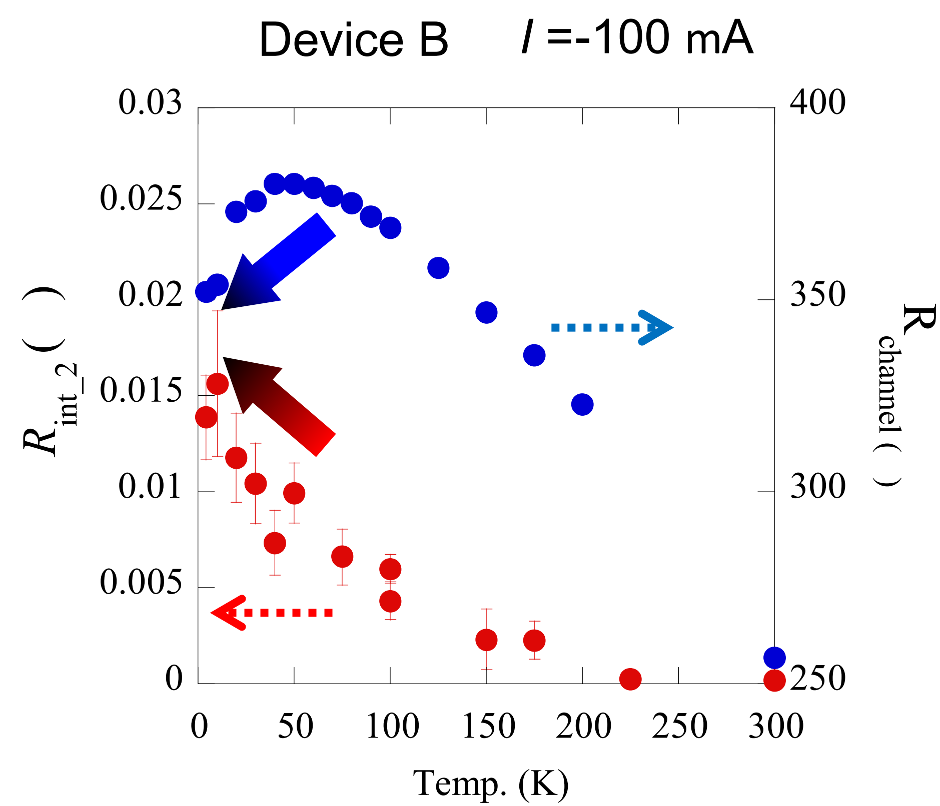

$$\frac{\rho_{BSTS}\ @4.2K}{\rho_{BSTS}\ @300K} = 1.07{\sim}1.43$$

⇒ Considerable surface conduction at 300 K.

Spin-charge coupled transport equations

PRL 105, 066802 (2010) PHYSICAL REVIEW LETTERS week ending 6 AUGUST 2010

Spin and Charge Transport on the Surface of a Topological Insulator

A. A. Burkov and D. G. Hawthorn
Department of Physics and Astronomy, University of Waterloo, Waterloo, Ontario N2L 3G1, Canada
(Received 12 May 2010; published 6 August 2010)

Spin drift-diffusion equations with spin-momentum locking

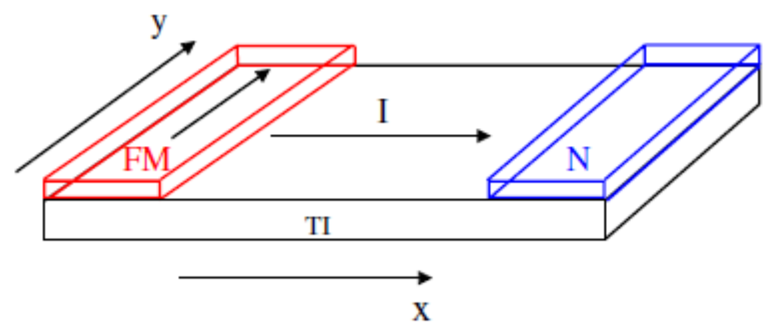

$$\frac{\partial N}{\partial t} = D\nabla^2 N + 2\Gamma(\hat{z}\times\nabla)\cdot S$$

$$\frac{\partial S^x}{\partial t} = \frac{D}{2}\frac{\partial^2 S^x}{\partial x^2} + \frac{3D}{2}\frac{\partial^2 S^x}{\partial y^2} + D\frac{\partial^2 S^y}{\partial x\partial y} - \frac{S^x}{\tau} + \Gamma(\hat{z}\times\nabla)_x N$$

$$\frac{\partial S^y}{\partial t} = \frac{D}{2}\frac{\partial^2 S^y}{\partial y^2} + \frac{3D}{2}\frac{\partial^2 S^y}{\partial x^2} + D\frac{\partial^2 S^x}{\partial x\partial y} - \frac{S^y}{\tau} + \Gamma(\hat{z}\times\nabla)_y N$$

Spin-charge coupled transport equations

Assuming $dS^x/dy=0, dS^y/dy=0$

$$D\frac{d^2N}{dx^2}+2\Gamma\frac{dS^y}{dx}=0 \qquad \frac{3D}{2}\frac{d^2S^y}{dx^2}-\frac{S^y}{\tau}+\Gamma\frac{dN}{dx}=0$$

Boundary conditions

$$J|_{x=\pm L/2}=\frac{I}{e} \qquad -\frac{3D}{2}\frac{dS^y}{dx}|_{x=-L/2}=\frac{I\eta}{e}$$

$$\frac{dS^y}{dx}|_{x=L/2}=0$$

Spin density along x direction

$$S^y(x)=\frac{I\eta}{ev_F}\sqrt{\frac{2}{3}}\frac{cosh\left[(2x-L)/\sqrt{3/2}l\right]}{sinh\left(2L/\sqrt{3/2}l\right)}-\frac{I}{2ev_F}$$

Spin-charge coupled transport equations

Spin dependent voltage due to spin momentum locking

$$V = \frac{1}{e\rho(\epsilon_F)} \int_{-L/2}^{L/2} \frac{dN}{dx} dx = \frac{2\pi I L}{e^2 k_F l} + \frac{4\pi I \eta}{e^2 k_F}$$

Charge current

$$\frac{\Delta V_2}{2} = \frac{4\pi I \hbar \eta}{e^2 k_F m}$$

$$\left(\frac{\Delta V_2}{I} = \Delta R_2 \right)$$

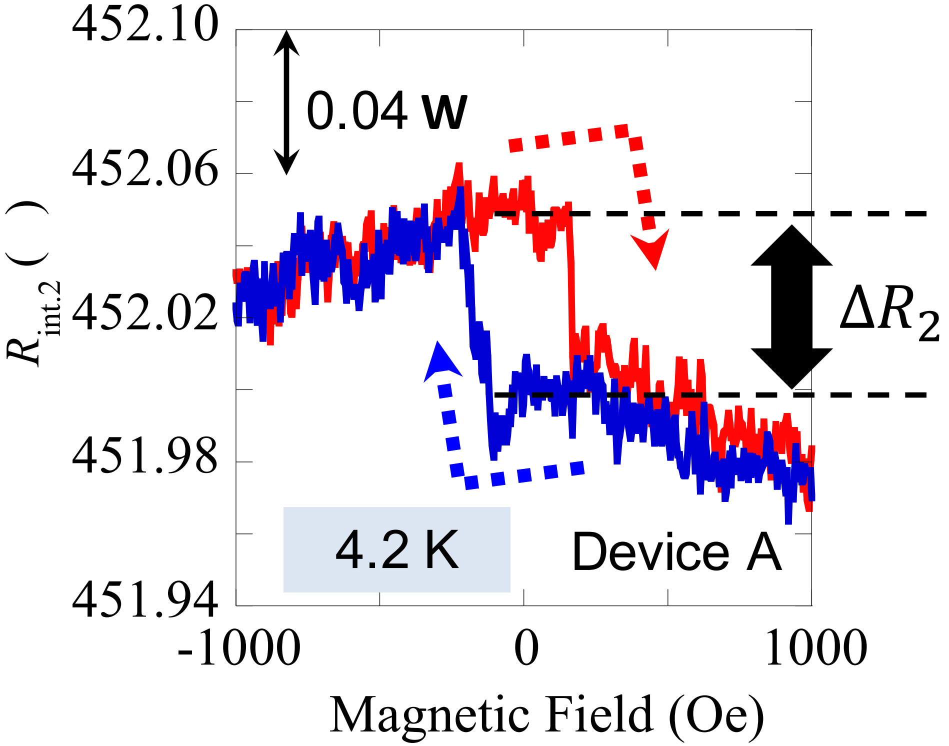

Bias current dependence of the spin signal

Spin dependent voltage due to spin momentum locking

$$V = \frac{1}{e\rho(\epsilon_F)} \int_{-L/2}^{L/2} \frac{dN}{dx} dx = \frac{2\pi I L}{e^2 k_F l} + \boxed{\frac{4\pi I \eta}{e^2 k_F}}$$

Charge current

$$\frac{\Delta V_2}{2} = \frac{4\pi I \hbar \eta}{e^2 k_F m}$$

$$\left(\frac{\Delta V_2}{I} = \Delta R_2 \right)$$

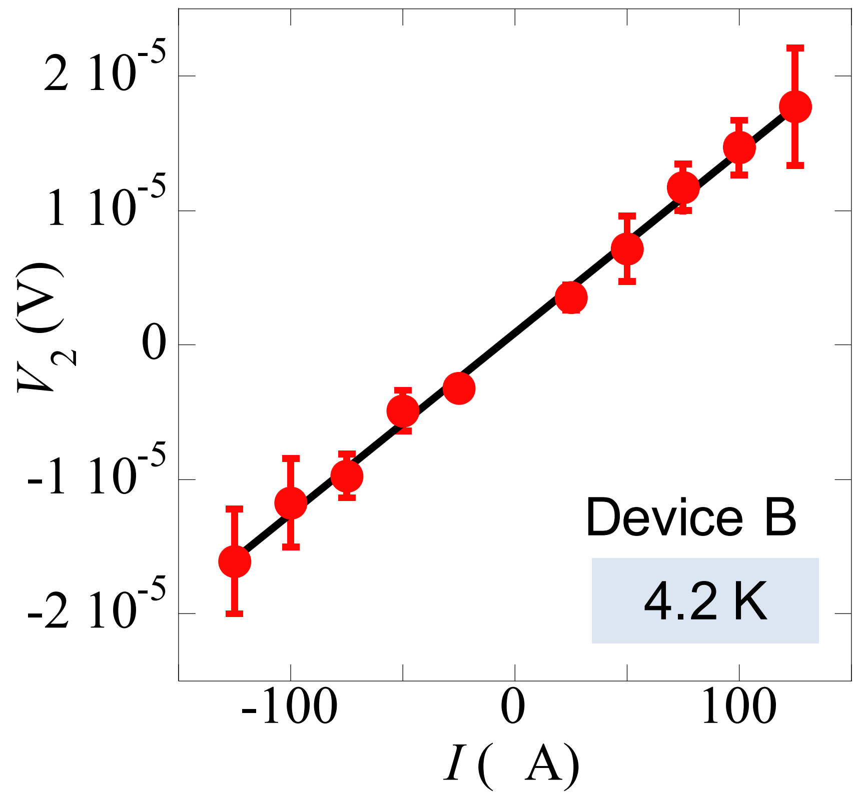

Estimation of spin injection and extraction efficiencies

Magnetoresistance

$$V = \frac{1}{e\rho(\epsilon_F)} \int_{-L/2}^{L/2} \frac{dN}{dx} dx = \frac{2\pi I L}{e^2 k_F l} + \frac{4\pi I \eta}{e^2 k_F}$$

100×10^{-6} [A=C/s]

1.05×10^{-34} [J・s=CV・s]

Spin polarization of injected current

$$\frac{\Delta V_2}{2} = \frac{4\pi I \hbar \eta}{e^2 k_F m}$$

Width of TI channel
2000 [nm] =2×10^4 [Å]

1.60×10^{-19} [C]

0.05~0.1 Å^{-1} from ARPES
(S. Kim et al., Phys. Rev. Lett. **112**, 136802 (2014).)

This study: 2*V*=4～40mV⇒*η*=0.05~0.5%

Charge current through the bottom surface

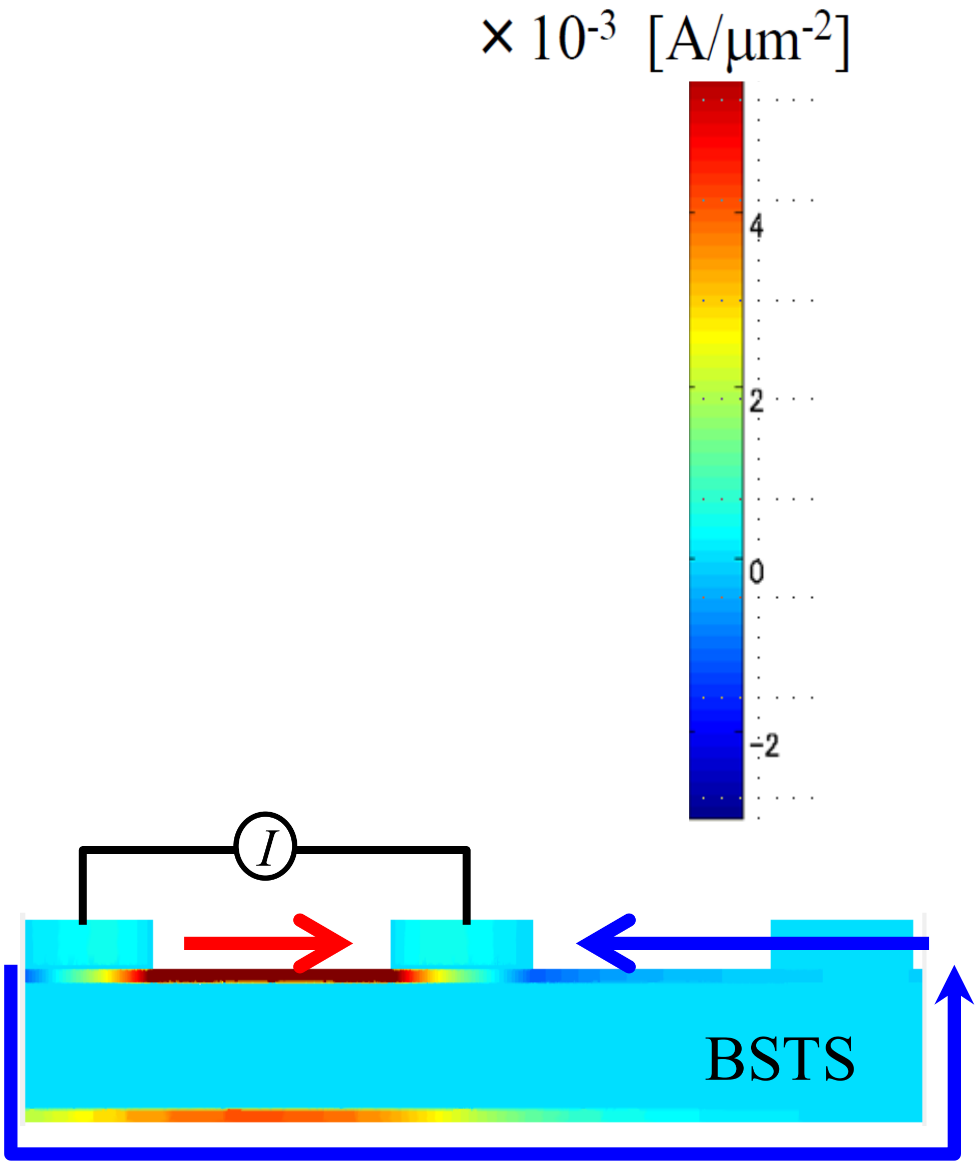

Charge current through the bottom surface

Charge current through the bottom surface

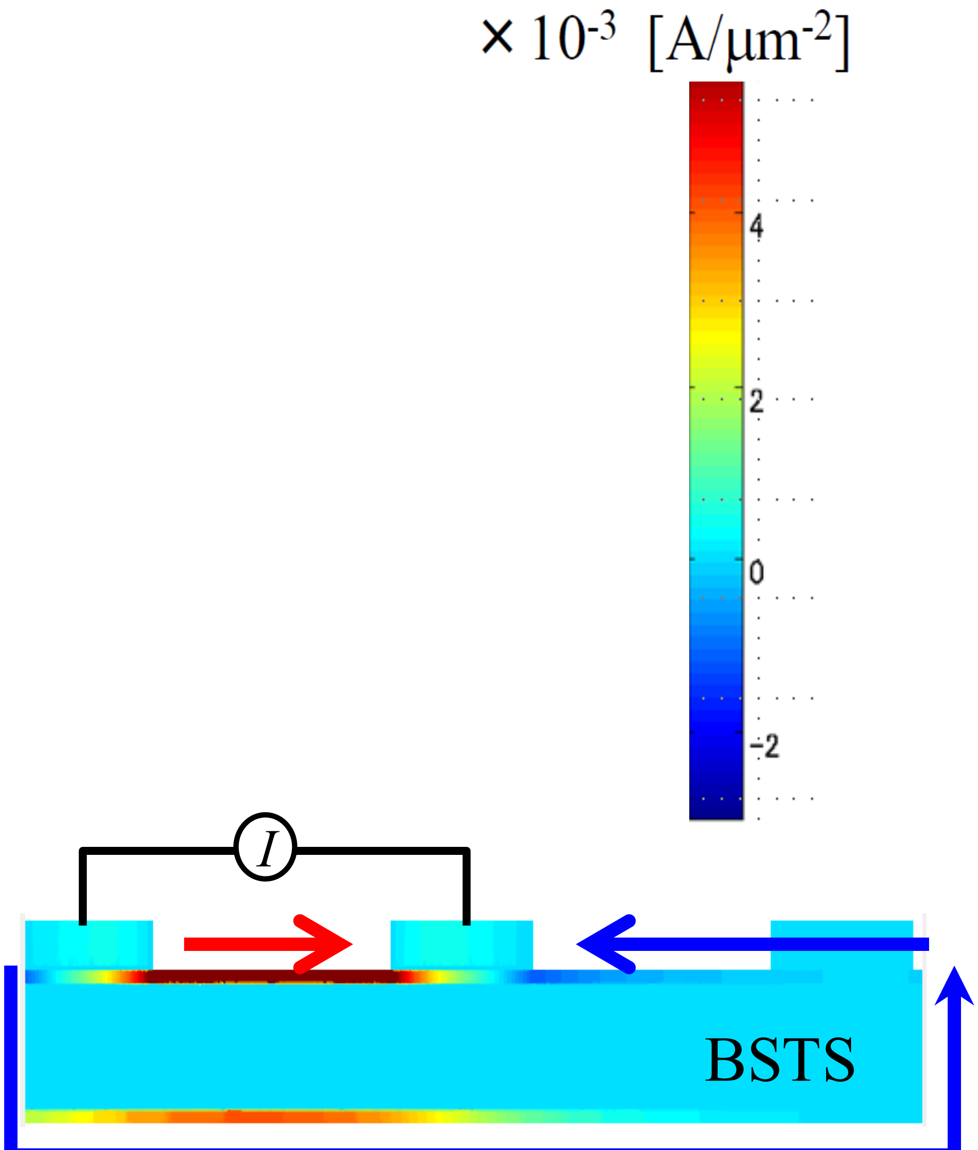

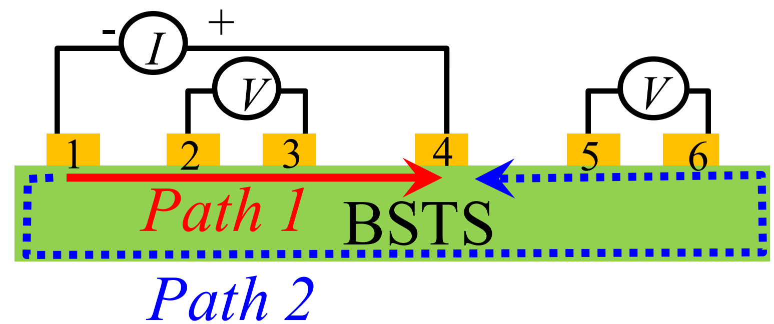

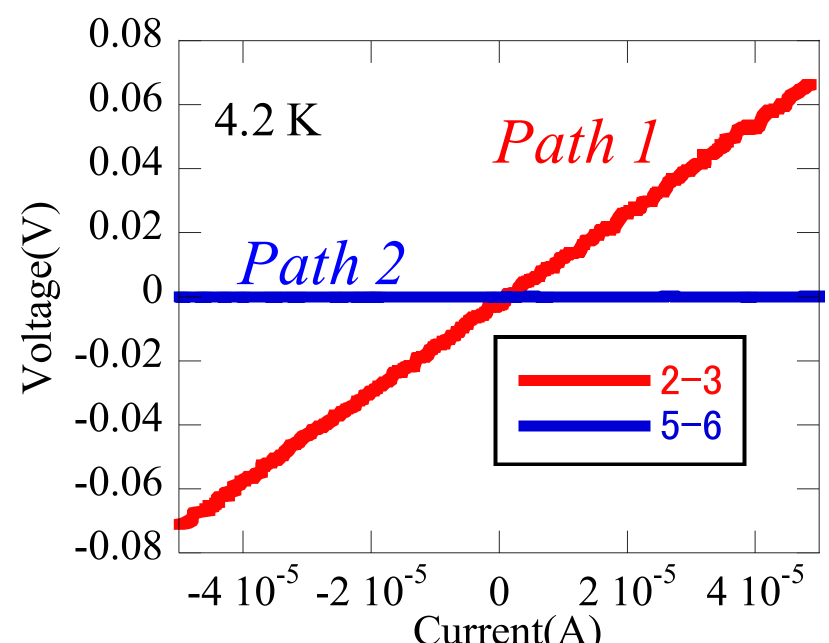

Charge current through the bottom surface

Effect of the interface resistance on the spin injection efficiency

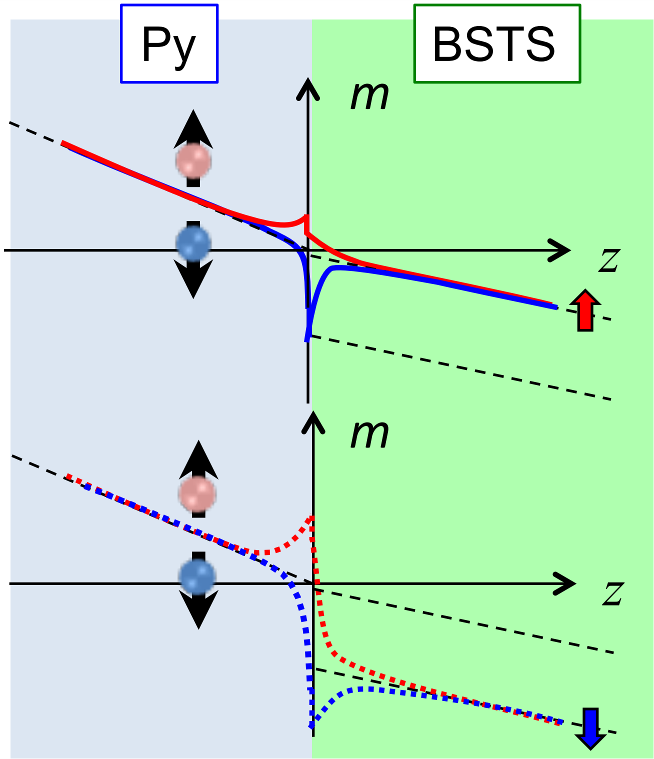

(in TI)

$$\mu_{\uparrow} = A\sigma_{+}^{-1} e^{\frac{z}{l}} + Bz + r_{i\uparrow} e J_{\uparrow},$$

$$\mu_{\downarrow} = -A\sigma_{-}^{-1} e^{\frac{z}{l}} + Bz + r_{i\downarrow} e J_{\downarrow},$$

(in Py)

$$\mu'_{\uparrow} = a\sigma_{\uparrow}^{-1} e^{-\frac{z}{l_F}} + bz + d,$$

$$\mu'_{\downarrow} = -a\sigma_{\downarrow}^{-1} e^{-\frac{z}{l_F}} + bz + d,$$

One dimensional spin drift-diffusion model

$$\frac{d}{e} = \left[\frac{r_i(1 - (P + P_F)\beta + PP_F))}{1 - \beta^2} + \frac{\left\{(\sigma_{+}^{-1} + \sigma_{-}^{-1})(P_F - P)l + \frac{4r_i(P_F - \beta)}{1 - \beta^2}\right\}\left\{(\sigma_{\uparrow}^{-1} + \sigma_{\downarrow}^{-1})(P_F - P)l_F + \frac{4r_i(\beta - P)}{1 - \beta^2}\right\}}{\ldots} \right] j$$

Effect of the interface resistance on the spin injection efficiency

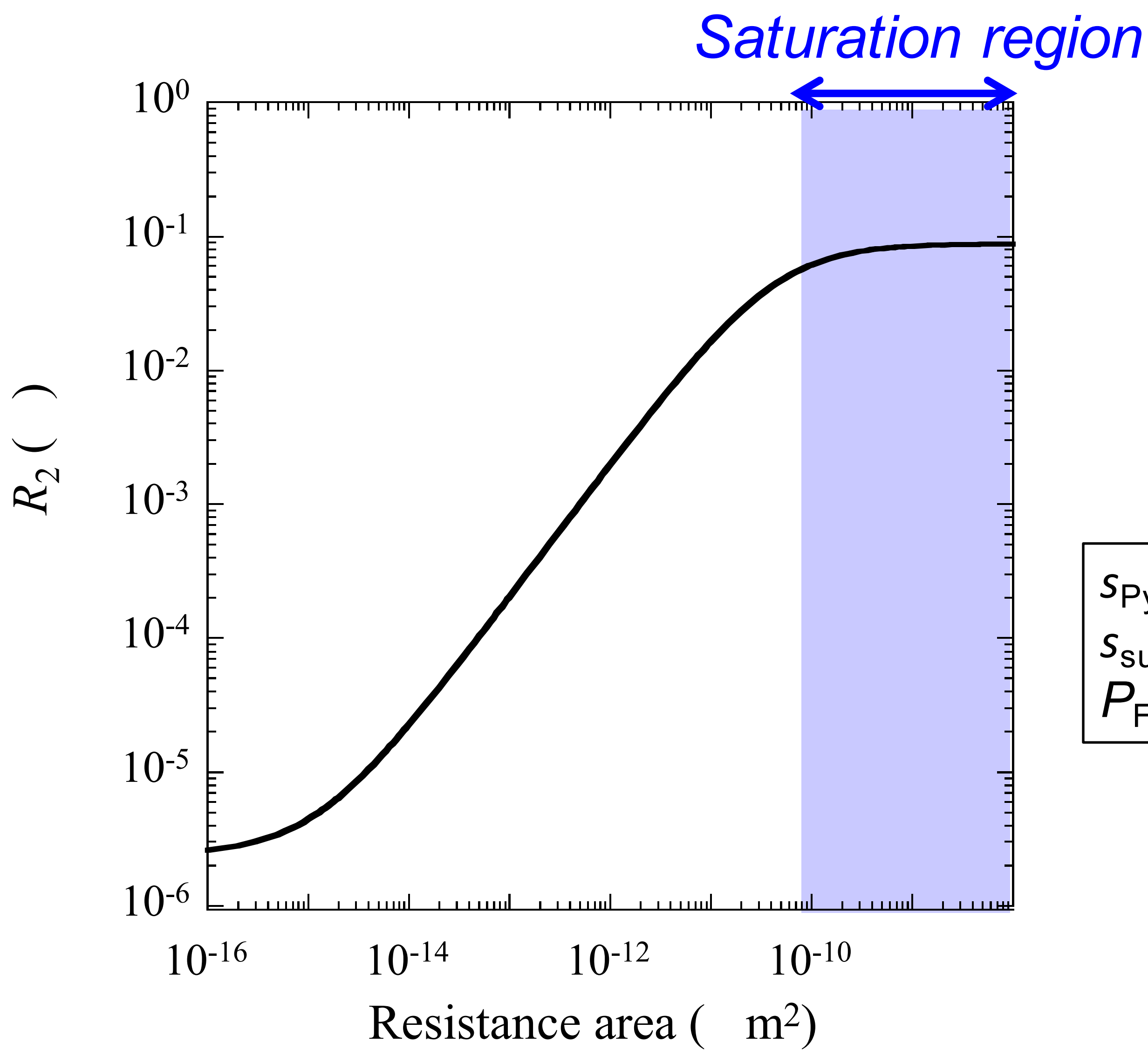

$s_{\mathrm{Py}} = 2.50\ \mathrm{W^{-1}mm^{-1}}$

$s_{\mathrm{sur\_iTI}} = 2.32 \times 10^{-2}\ \mathrm{W^{-1}mm^{-1}}$

$P_{\mathrm{F}} = 0.5\ \%$

Effect of the interface resistance on the spin injection efficiency

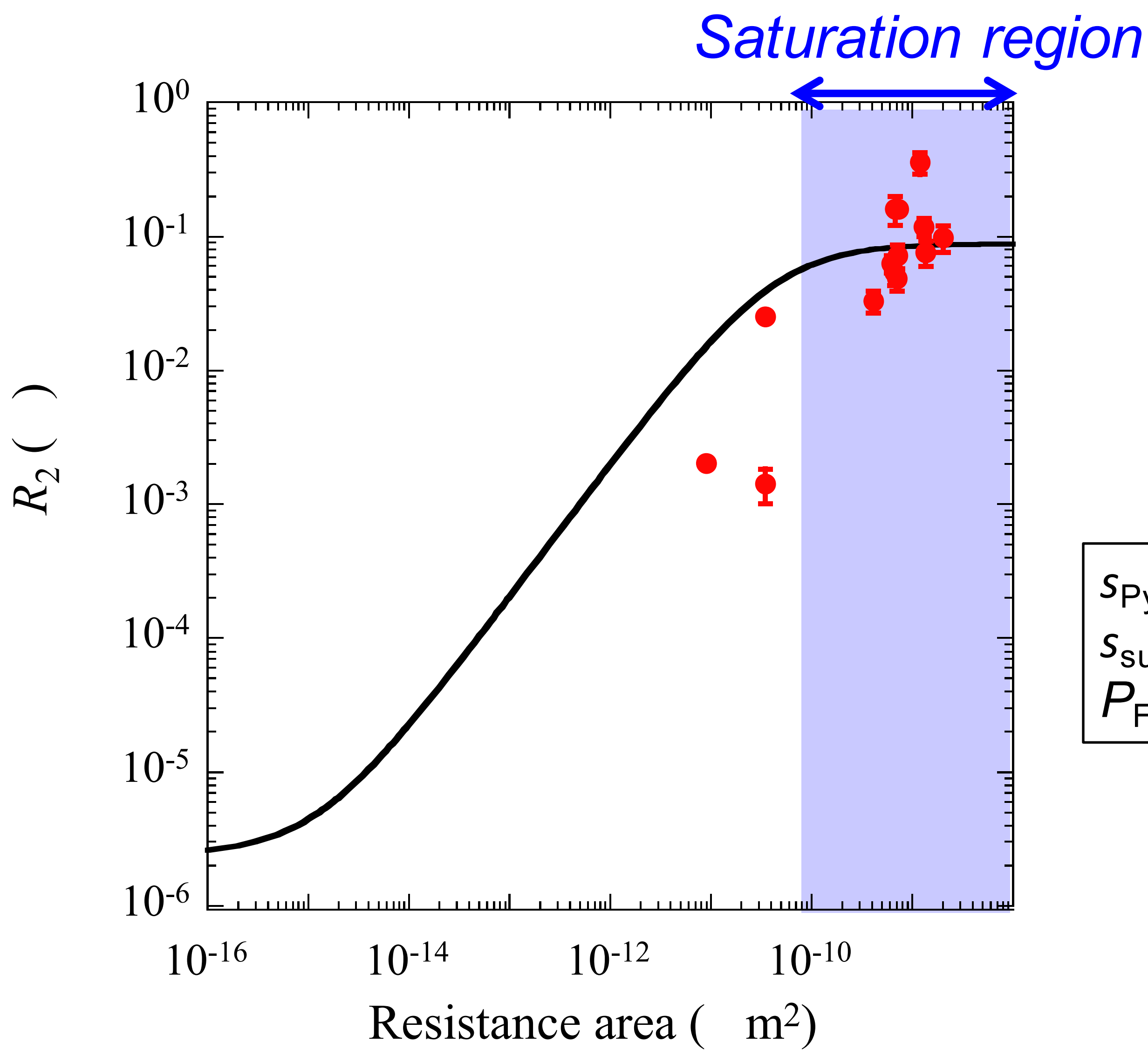

s_{Py} = 2.50 $W^{-1}mm^{-1}$
s_{sur_iTI} = 2.32 × 10^{-2} $W^{-1}mm^{-1}$
P_F = 0.5 %

⇒ The conductance mismatch problem is not crucial issue.

Possible origin of the low spin injection efficiency

① Unoptimized spin injection and extraction geometry

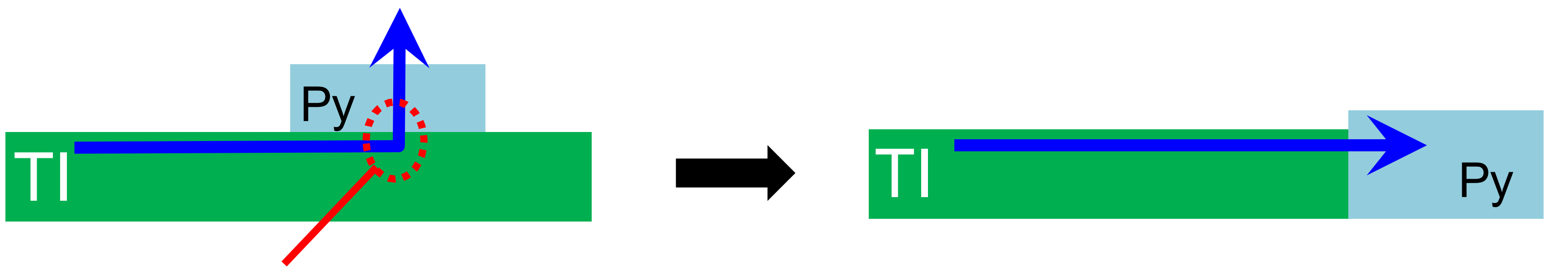

Carrier momentum change
⇒Spin angular momentum change??

② Low quality Py/TI interface (e.g. Intermixing TI and FM)

⇒ ・ Insertion of MgO or Al_2O_3 tunnel barrier
・ Improvement of device fabrication procedure
e.g., Ferromagnetic materials,
Low temperature deposition

Summary

We have demonstrated the electrical injection and extraction of the spin polarized current due to spin-momentum locking of bulk-insulating topological insulator $Bi_{1.5}Sb_{0.5}Te_{1.7}Se_{1.3}$

- ✓ Local magnetoresistance
- ✓ Spin injection/extraction efficiency: 0.05~0.5% ($BSTS>>Bi_2Se_3$)
- ✓ Detectable temperature: 4.2~200 K

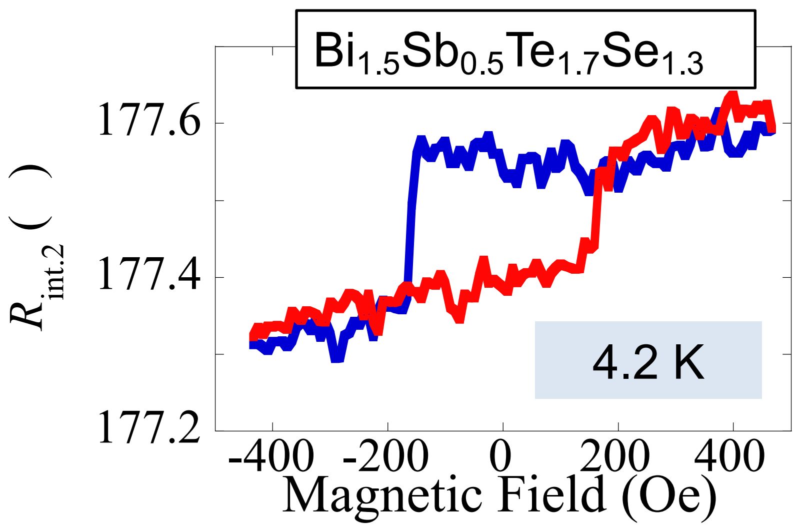

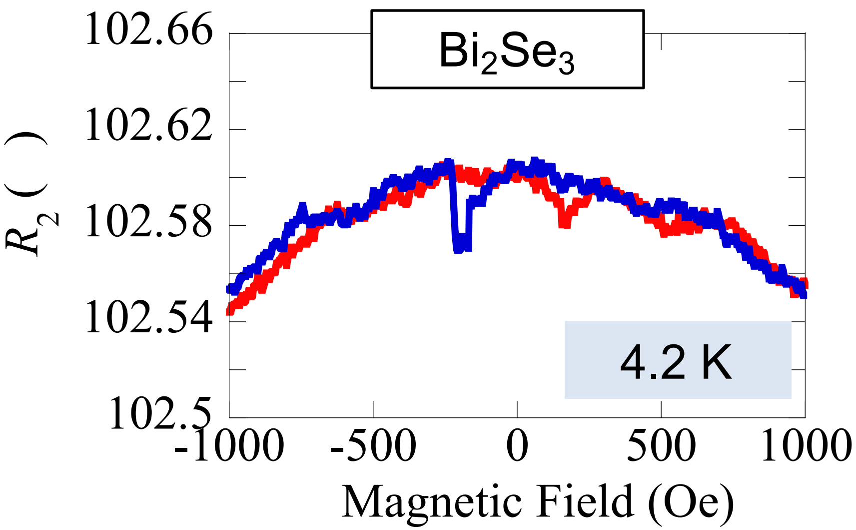

Y. Ando et al., Nano Lett. 14, 6226(2014).

Spin Polarization in TI

$$P = \frac{j}{j_0} = \frac{j e \mu_0^2}{4\pi\hbar^2 v_F} = 16.7\%$$

$$\left(\begin{aligned} \mu_0 &= 100\, meV \\ j &= \frac{1\times10^{-4}[A]}{2\times10^{-6}[m]} = 50[\mathrm{A}m^{-1}] \\ j_0 &= \frac{1.6\times10^{-19}[A]0.1^2[eV]}{4\pi\times(6.58\times10^{-16})^2\,[eVs]} = 300[\mathrm{A}m^{-1}] \end{aligned} \right)$$

Spin accumulation measurements

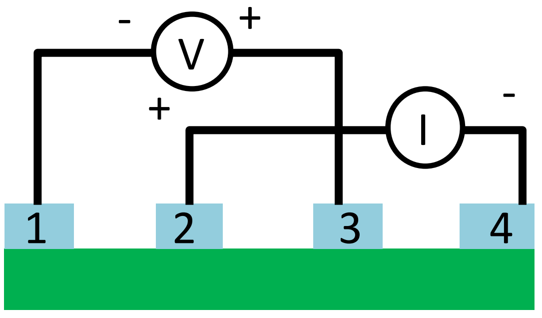

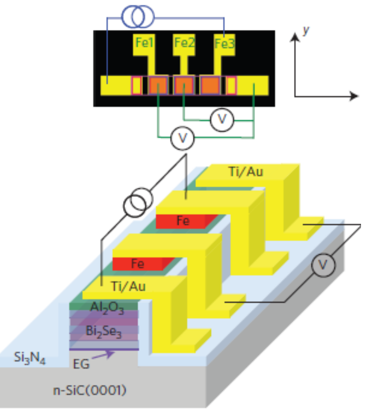

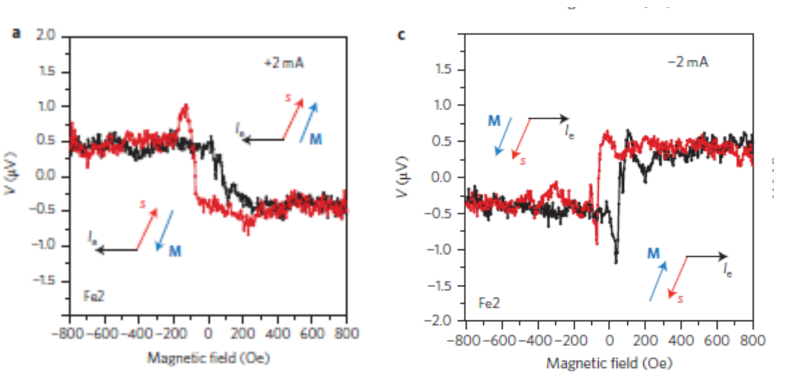

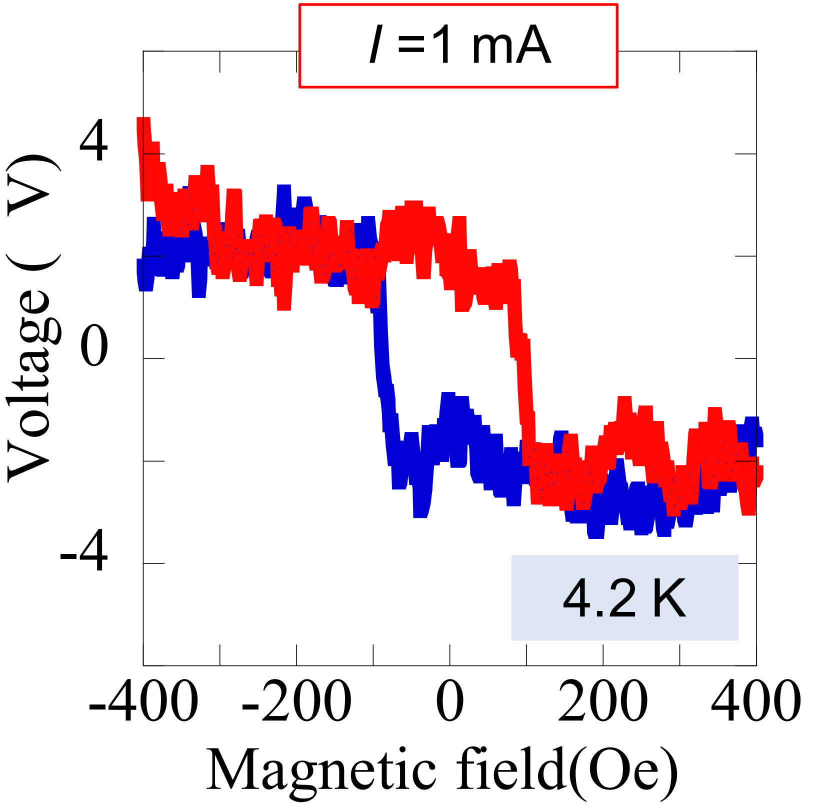

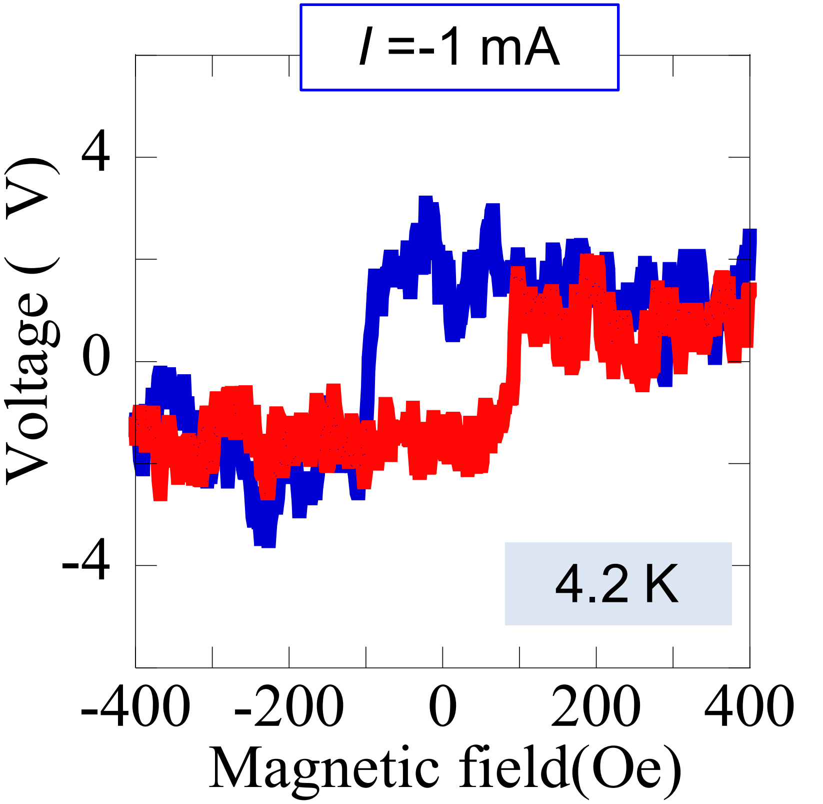

Charge current through the bottom and side surface

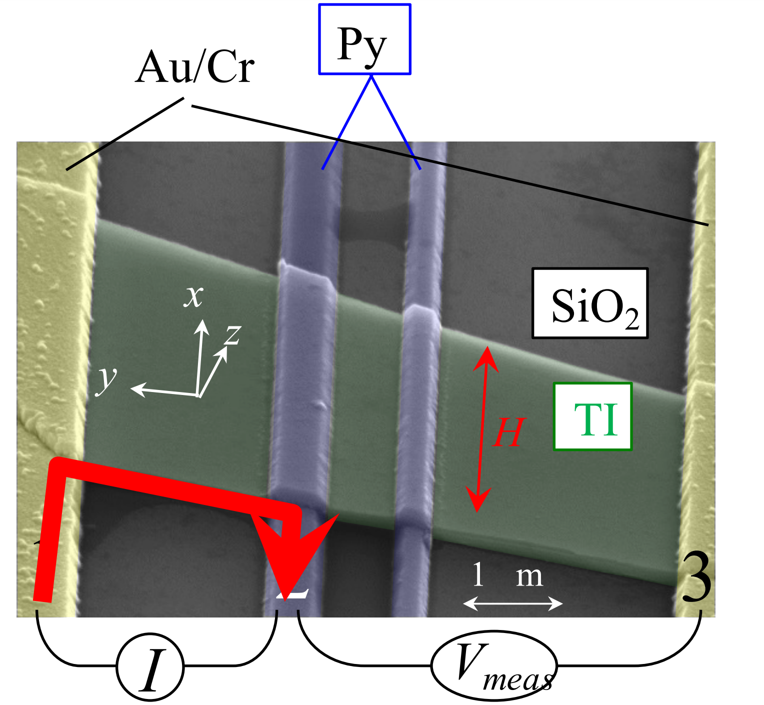

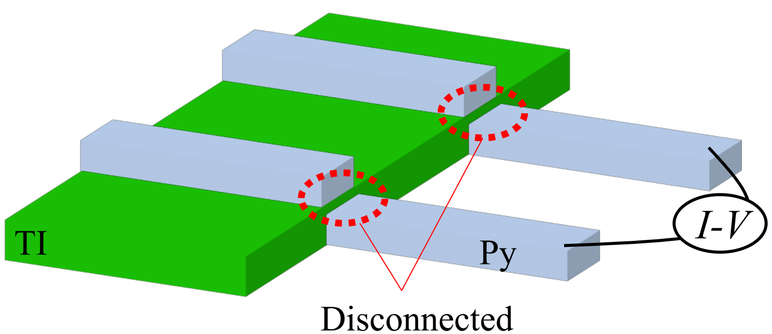

⇒ No electric conduction

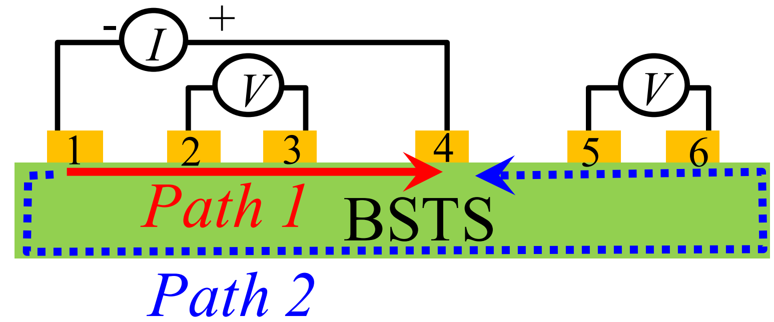

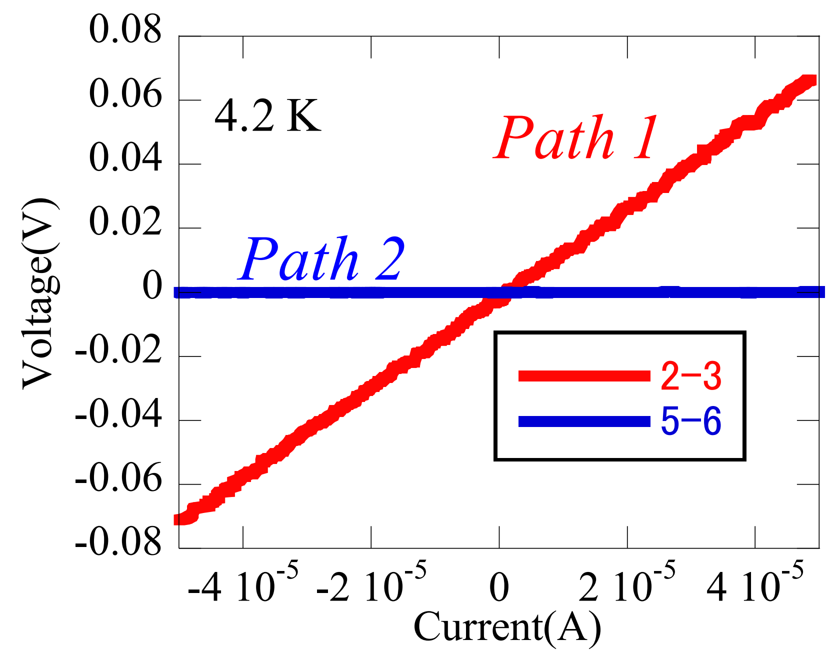

Bias current dependence of DV_2

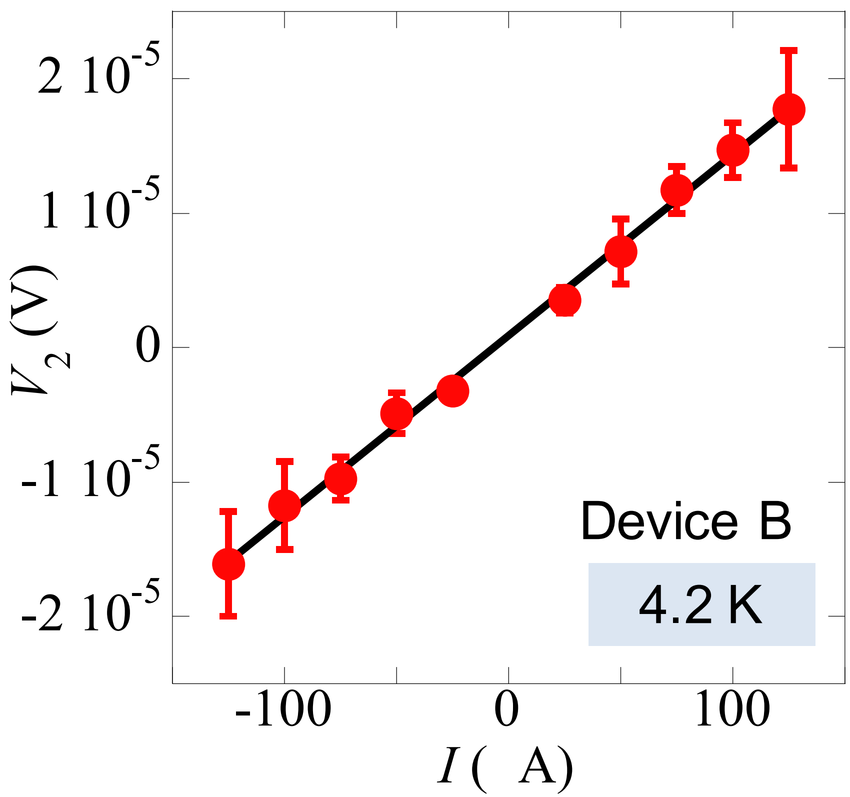

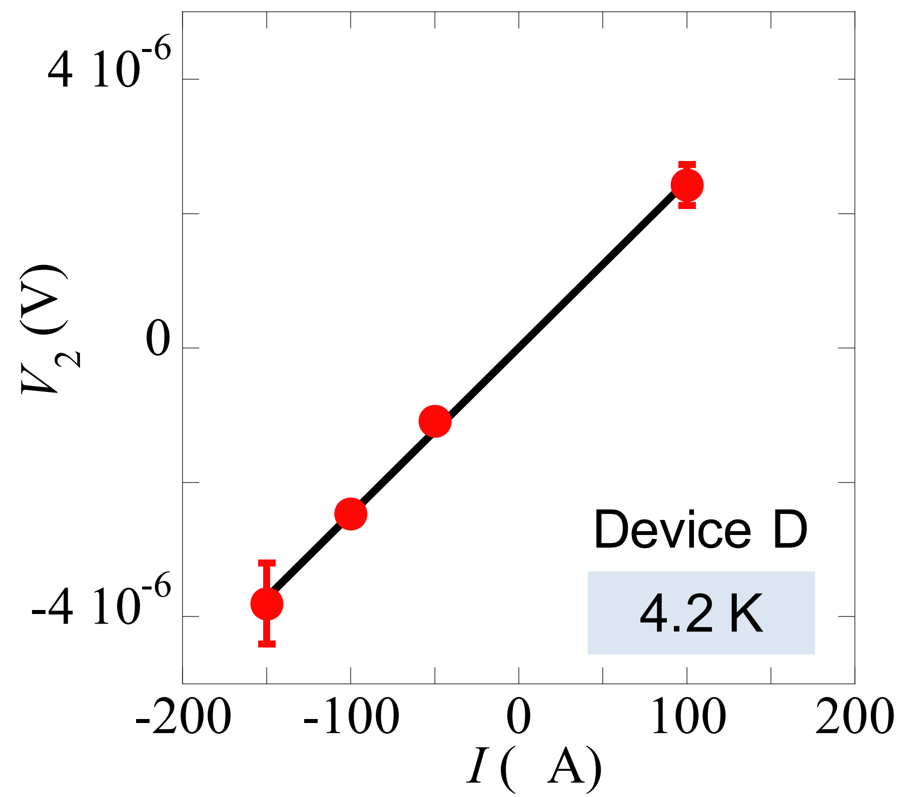

A linear relationship between DV_2 vs I

R_2-H curves of Bi_2Se_3 devices

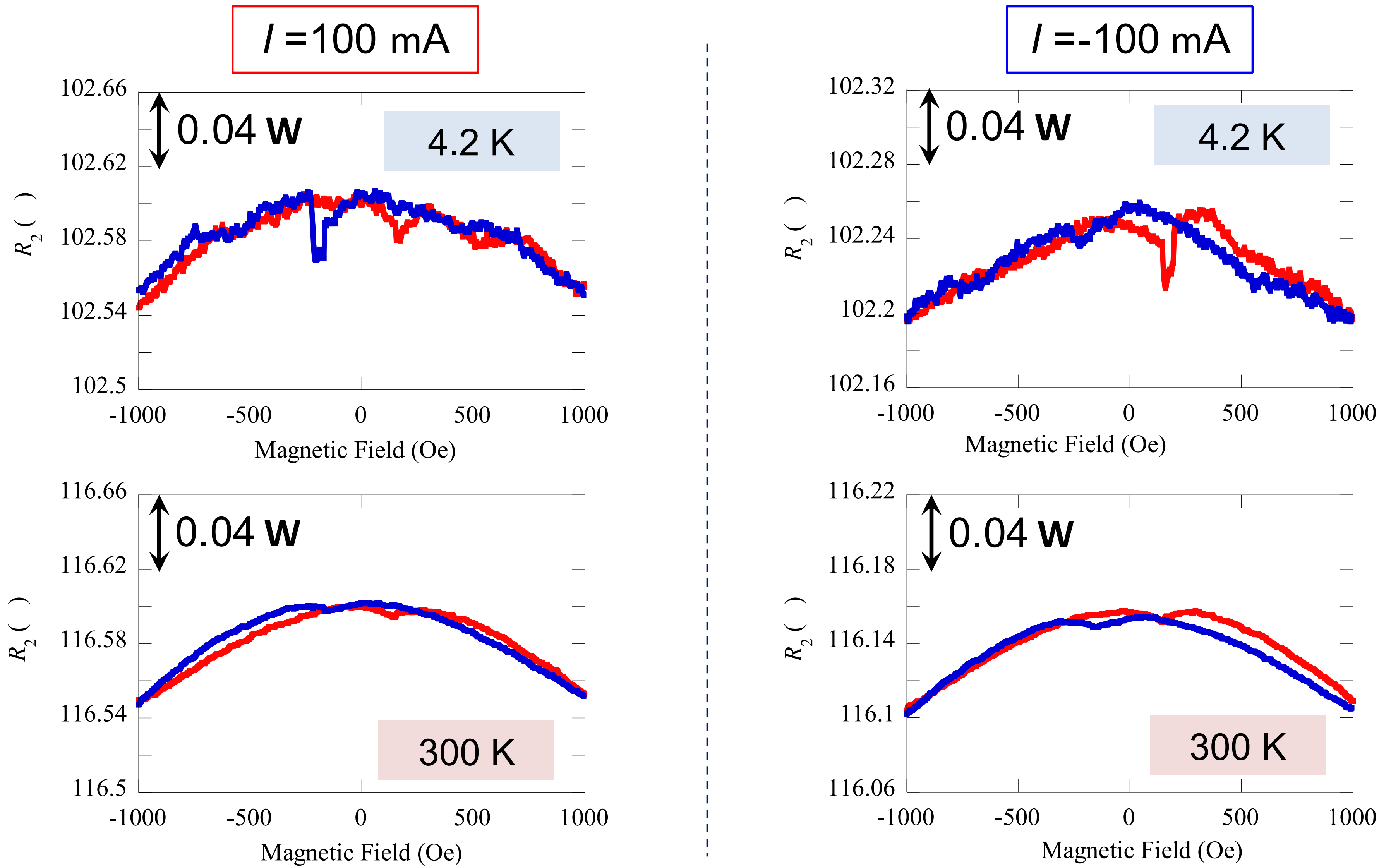

No rectangular hysteresis signals

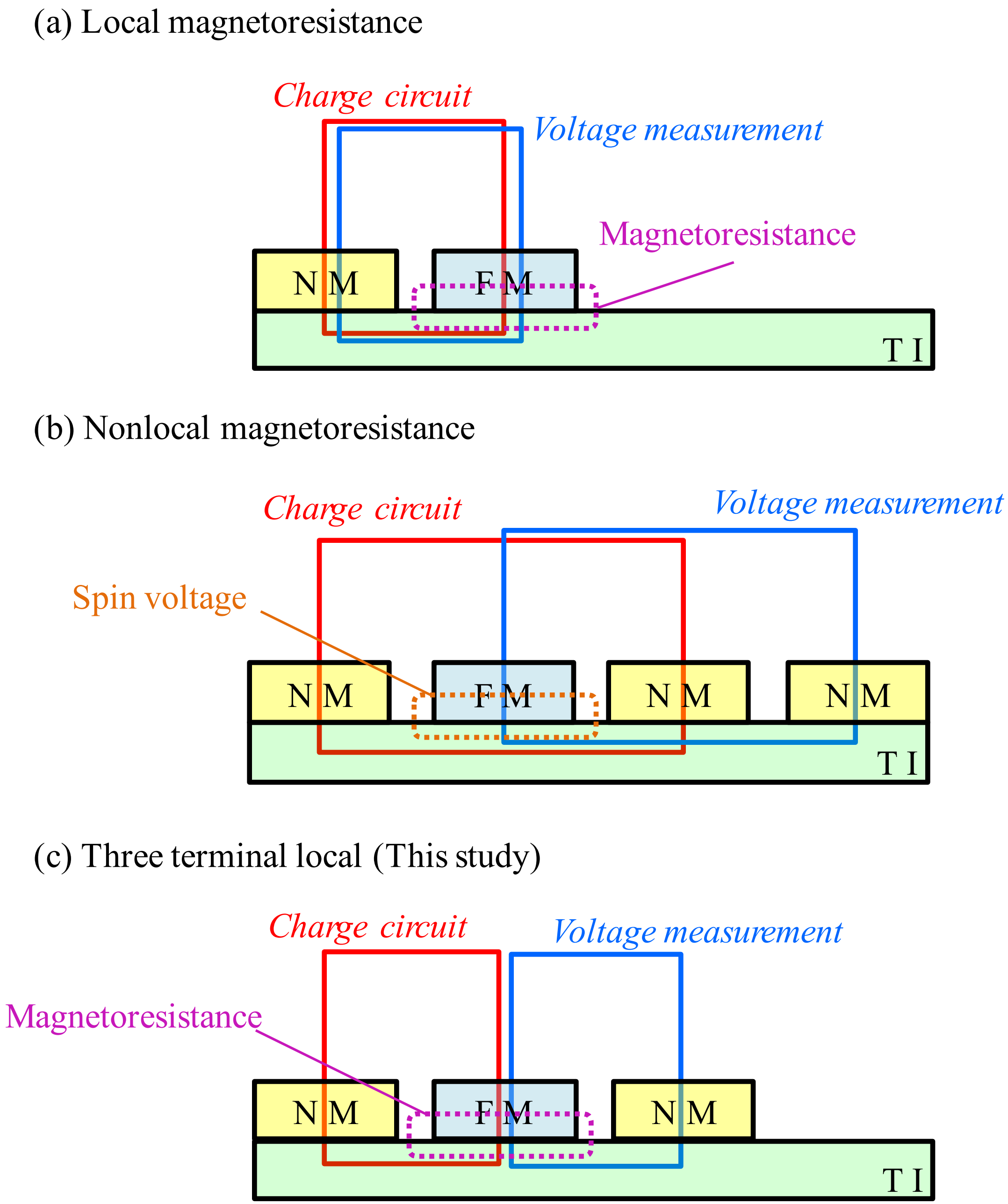
(a) Local magnetoresistance
Charge circuit
Voltage measurement
Magnetoresistance
N M
F M
T I
(b) Nonlocal magnetoresistance
Charge circuit
Voltage measurement
Spin voltage
N M
F M
N M
N M
T I
(c) Three terminal local (This study)
Charge circuit
Voltage measurement
Magnetoresistance
N M
F M
N M
T I

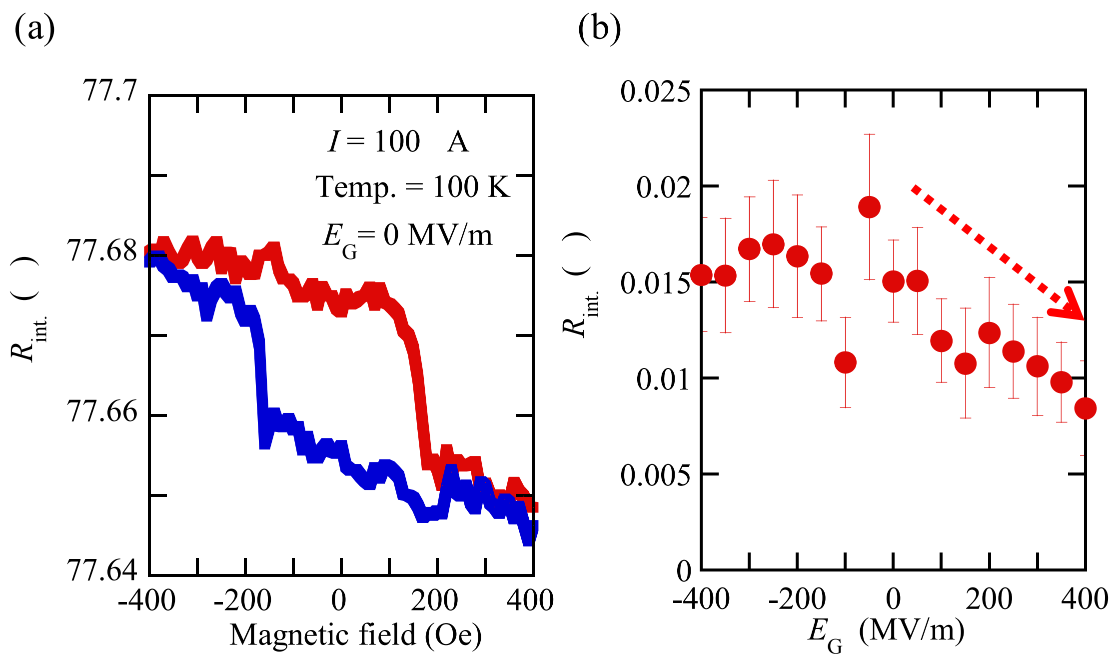
(a)
(b)
77.7
77.68
77.66
77.64
$R_{int.}$ ( )
I = 100 A
Temp. = 100 K
E_G = 0 MV/m
-400
-200
0
200
400
Magnetic field (Oe)
0.025
0.02
0.015
0.01
0.005
0
$R_{int.}$ ( )
-400
-200
0
200
400
E_G (MV/m)

Temperature dependence of DR_2 (Device B)

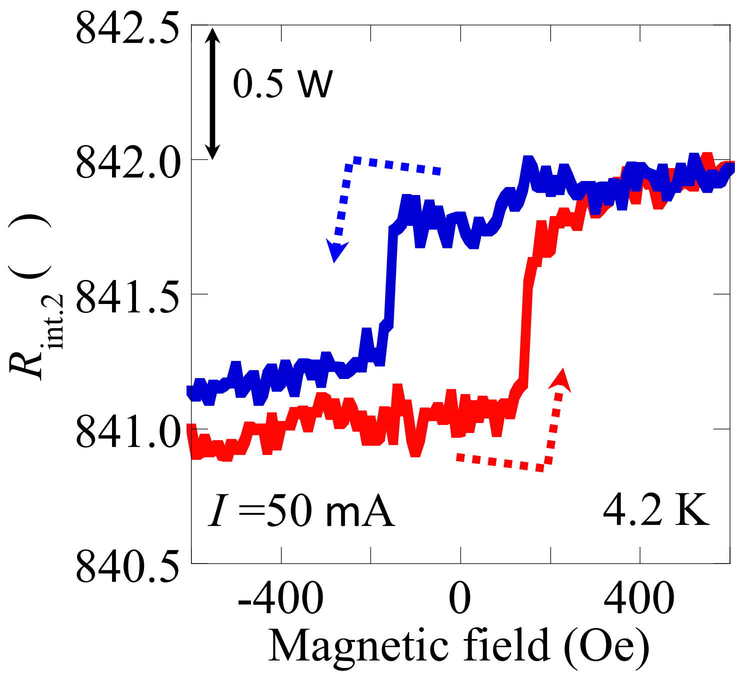

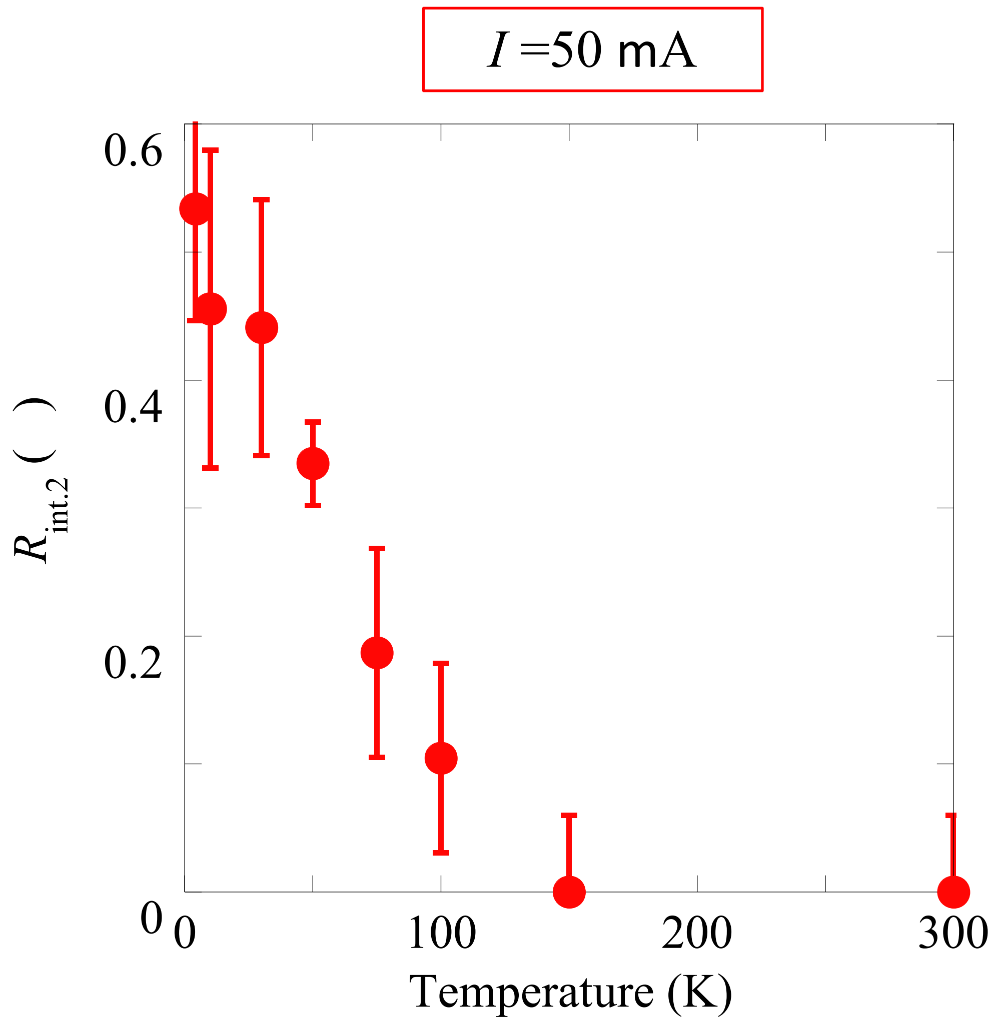

Rectangular hysteresis signals disappeared at 150 K

A technical issue

- High charge current density (> 100 ~ 1000 mA)
- Large interface and channel resistances

⇒ The TI devices were easily broken.

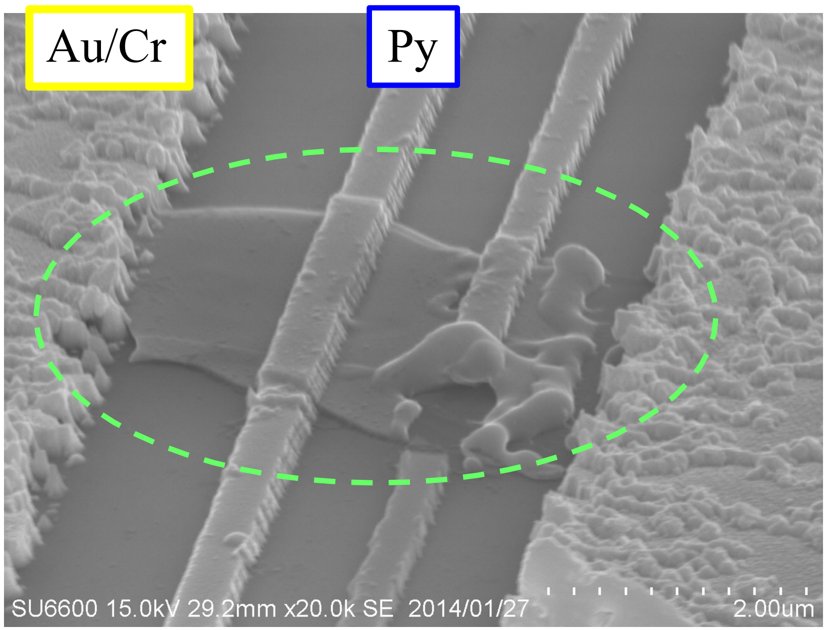

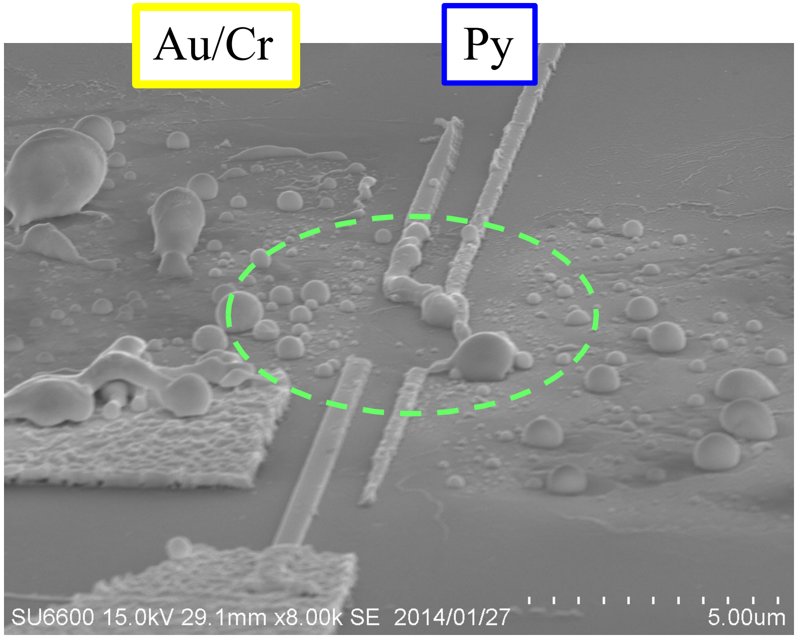

Spurious effects expected in FM/TI devices

Magnetization & charge current

- ✓ Anisotropic Magnetoresistance (AMR)
- ✓ Planar Hall effect (PHE)
- ✓ Anomalous Hall effects (AHE)
- ✓ Lorenz MR
- ✓ Tunneling Anisotropic Magnetoresistance (TAMR)

Magnetization & Thermal gradient

- ✓ Anomalous Nernst effects (ANE)
- ✓ Spin Seebeck effect (SSE)

….etc

A strong TI dependence and temperature dependence of the rectangular signals cannot be explained as a result of the spurious effects.

Spurious effects expected in FM/TI devices

- ✓ Anisotropic Magnetoresistance (AMR)

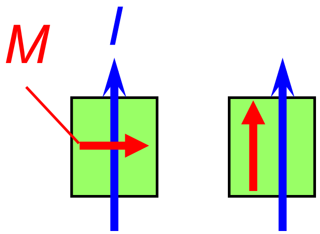

$$r_{M//I} \neq r_{M\perp I}$$

- ✓ Planar Hall effect (PHE)

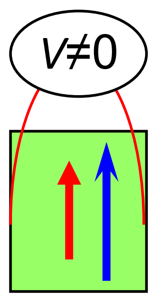

- ✓ Anomalous Hall effect (AHE)

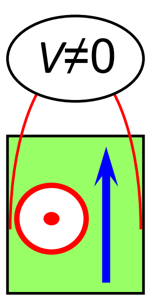

Difference between BS and BSTS devices ?????

Spurious effects expected in FM/TI devices

- ✓ Lorenz MR

Disappearance of the rectangular signals at 300 K
&
Clear AMR signals at 300K ⇒???

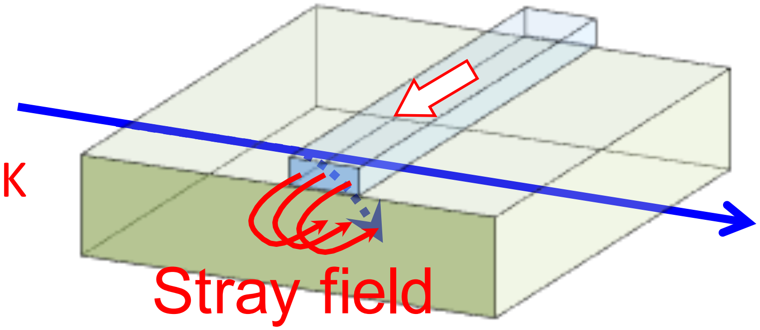

- ✓ Tunneling Anisotropic Magnetoresistance (TAMR)

Origin
: An anisotropic density of states
[C. Gould et al., PRL **93**, 117203(2004).]

Interference of Rashba and Dresselhaus spin-orbit interactions
[L. Moser et al., PRL **99**, 056601(2007).]

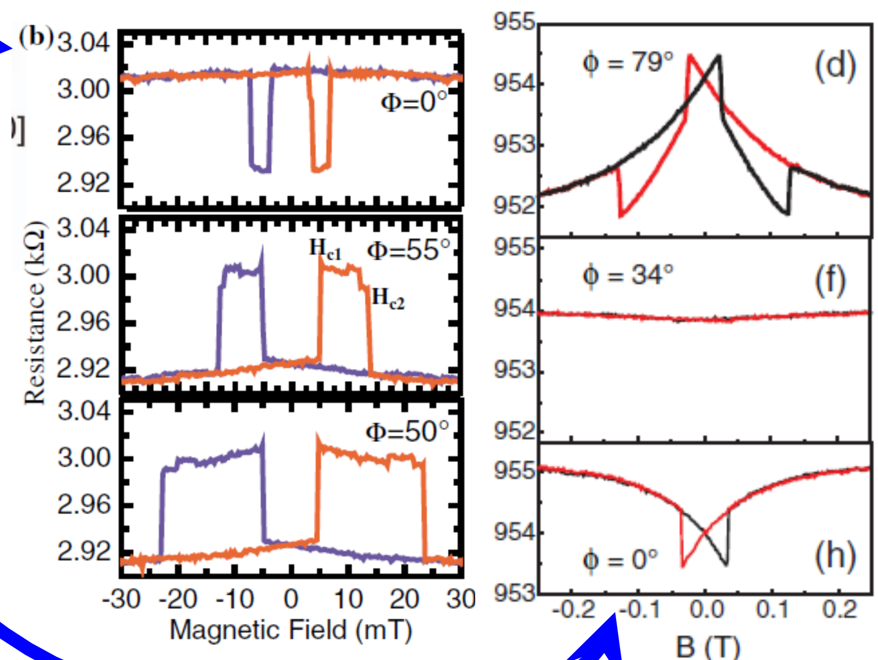

Discrepancy between AMR signals and Rectangular signals ??

Possible origin of the low spin injection efficiency

- Low spin injection efficiency (η=0.0005~0.005)

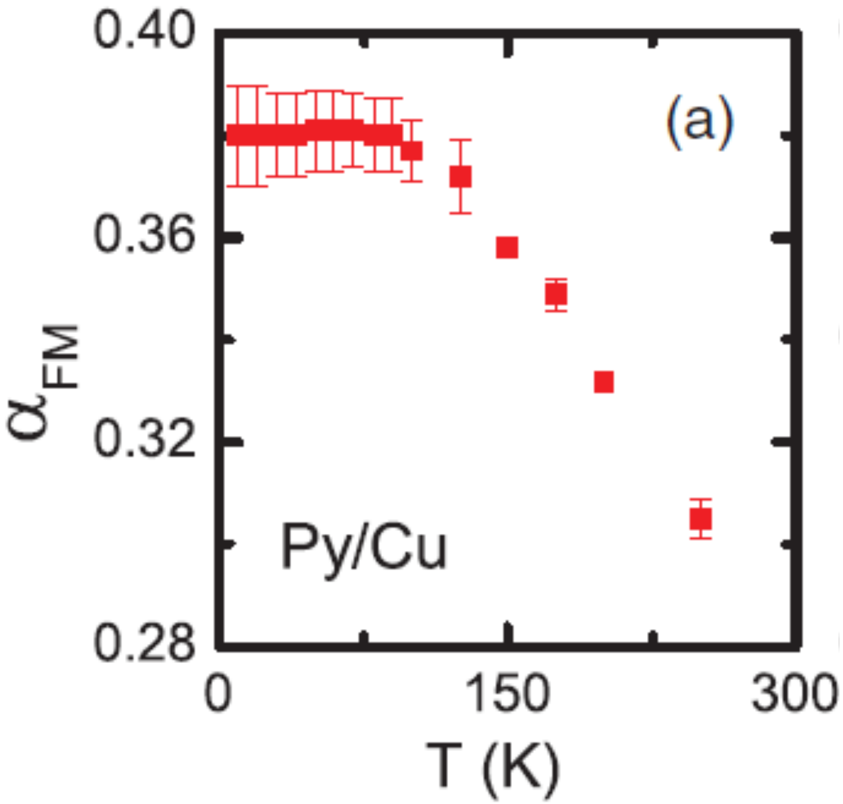

Spin polarization of Py

✓ Py/metal interface 0.2~0.4

✓ Small temperature dependence

E. Villamor Phys. Rev. B **88**, 184411 (2013).

Possible origin of the low spin injection efficiency

(in TI)

$$\mu_\uparrow = A\sigma_+^{-1} e^{\frac{z}{l}} + Bz + r_{i\uparrow} e J_\uparrow,$$

$$\mu_\downarrow = -A\sigma_-^{-1} e^{\frac{z}{l}} + Bz + r_{i\downarrow} e J_\downarrow\,,$$

(in Py)

$$\mu'_\uparrow = a\sigma_\uparrow^{-1} e^{-\frac{z}{l_F}} + bz + \boxed{d},$$

$$\mu'_\downarrow = -a\sigma_\downarrow^{-1} e^{-\frac{z}{l_F}} + bz + \boxed{d}\,,$$

One dimensional spin drift-diffusion model

$$\frac{d}{e} = \left[\frac{r_i(1-(P+P_F)\beta + PP_F))}{1-\beta^2} + \frac{\left\{(\sigma_+^{-1}+\sigma_-^{-1})(P_F-P)l + \frac{4r_i(P_F-\beta)}{1-\beta^2}\right\}\left\{(\sigma_\uparrow^{-1}+\sigma_\downarrow^{-1})(P_F-P)l_F + \frac{4r_i(\beta-P)}{1-\beta^2}\right\}}{4\left\{(\sigma^{-1}+\sigma^{-1})l + (\sigma^{-1}+\sigma^{-1})l_F + \frac{4r_i}{\ldots}\right\}}\right] j$$

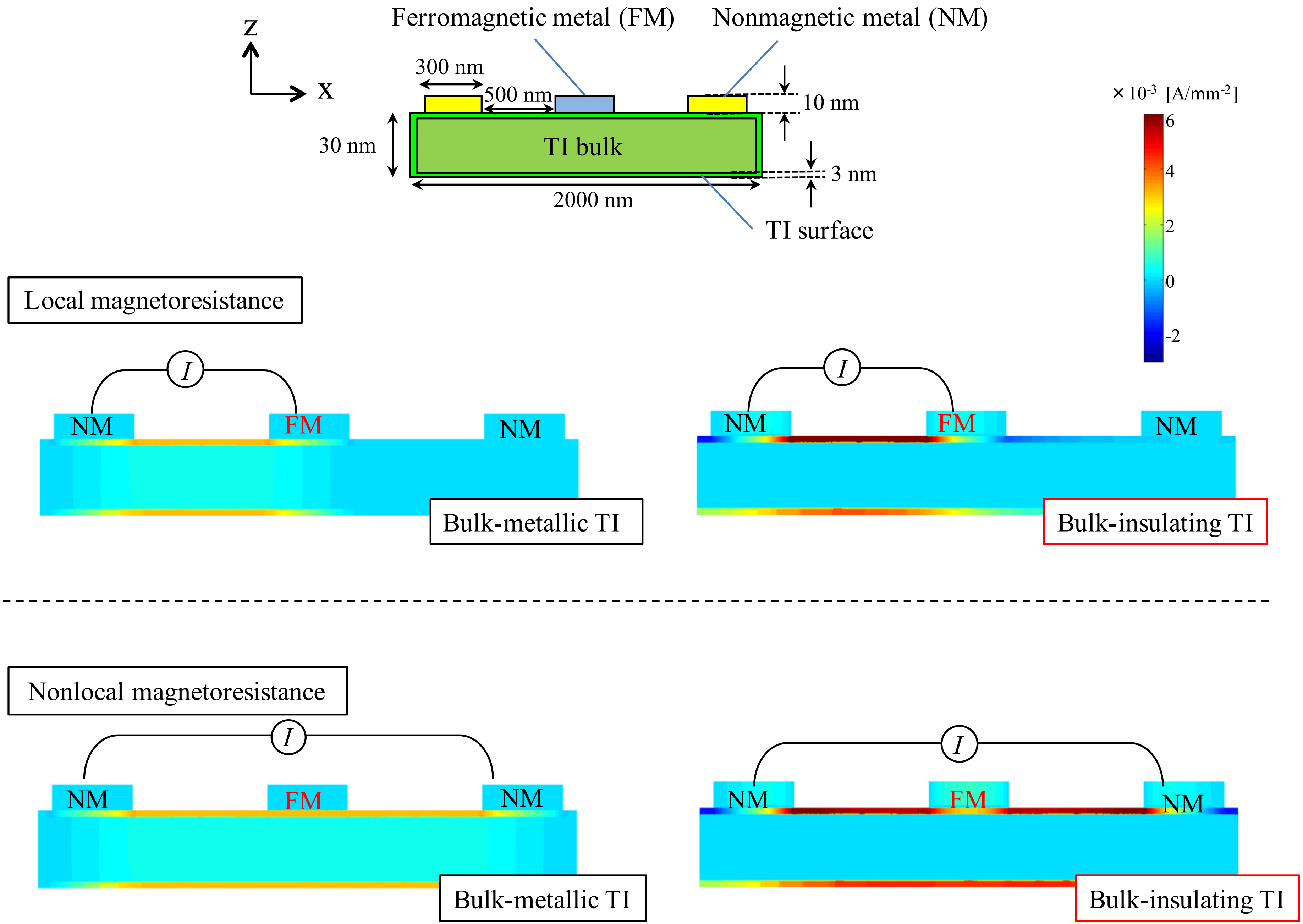
Z
X
Ferromagnetic metal (FM)
Nonmagnetic metal (NM)
300 nm
500 nm
10 nm
30 nm
TI bulk
3 nm
2000 nm
TI surface
× 10-3 [A/mm-2]
6
4
2
0
-2
Local magnetoresistance
I
NM
FM
NM
Bulk-metallic TI
I
NM
FM
NM
Bulk-insulating TI
Nonlocal magnetoresistance
I
NM
FM
NM
Bulk-metallic TI
I
NM
FM
NM
Bulk-insulating TI

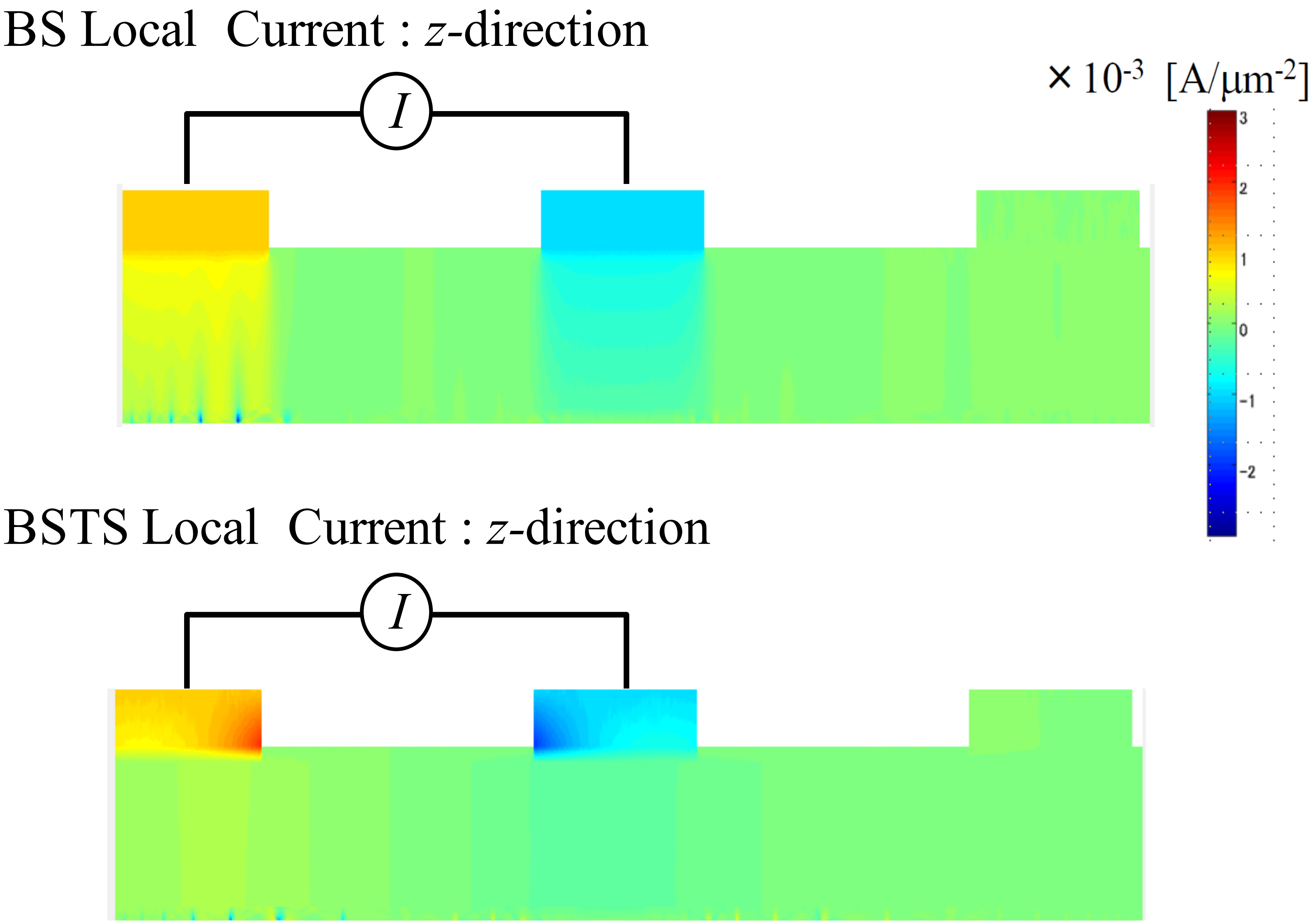
BS Local Current : z-direction
I
× 10-3 [A/μm-2]
3
2
1
0
−1
−2
BSTS Local Current : z-direction
I

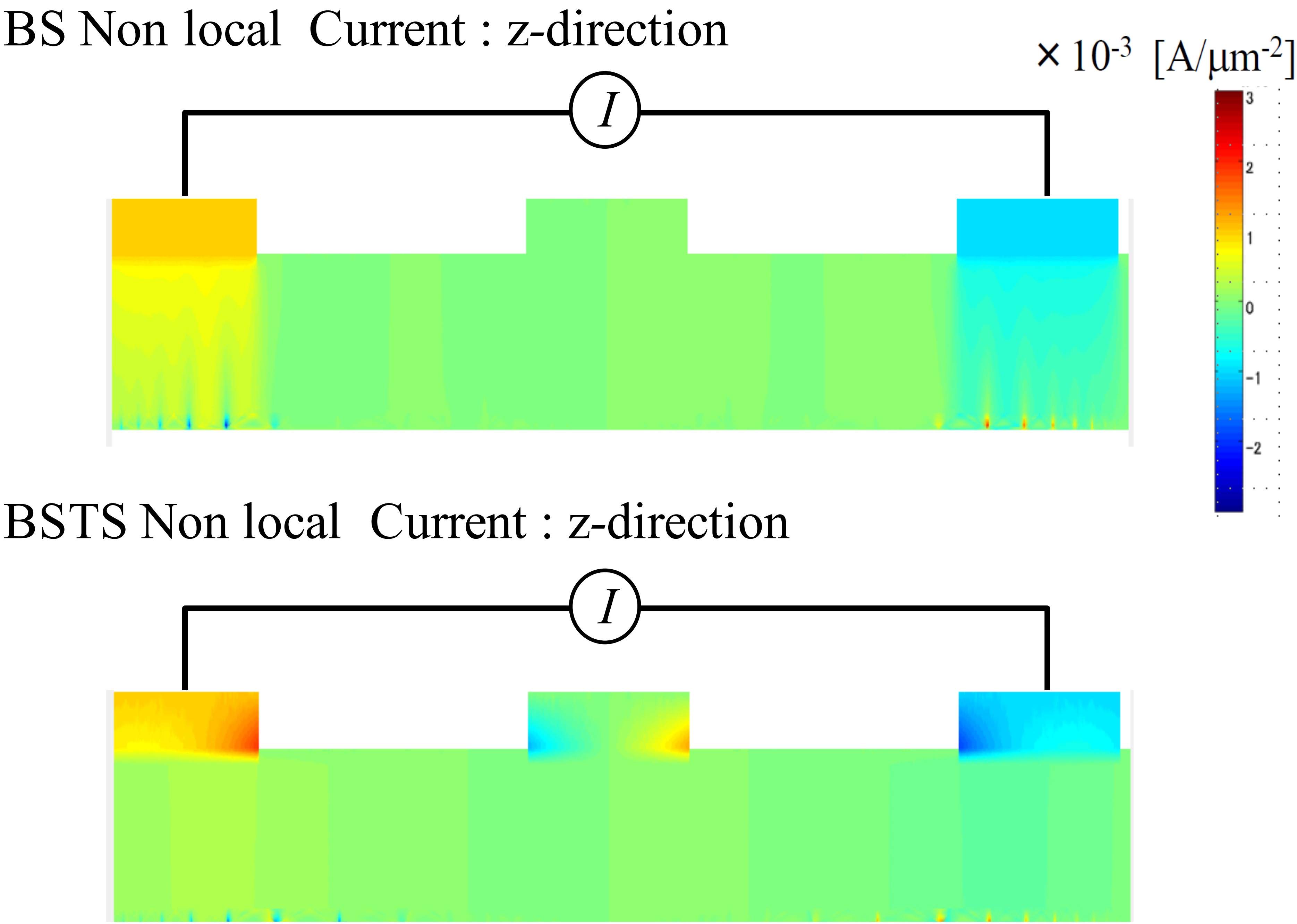

BS Non local Current : z-direction
× 10-3 [A/μm-2]
I
3
2
1
0
-1
-2
BSTS Non local Current : z-direction
I

BSTS Local Current : x-direction real scale